

RUTHENIUM(0) NANOPARTICLES SUPPORTED ON HAFNIA:
A HIGHLY ACTIVE AND LONG-LIVED CATALYST IN HYDROLYTIC
DEHYDROGENATION OF AMMONIA BORANE

A THESIS SUBMITTED TO
THE GRADUATE SCHOOL OF NATURAL AND APPLIED SCIENCES
OF
MIDDLE EAST TECHNICAL UNIVERSITY

BY

ELİF BETÜL KALKAN

IN PARTIAL FULFILLMENT OF THE REQUIREMENTS
FOR
THE DEGREE OF MASTER OF SCIENCE
IN
CHEMISTRY

SEPTEMBER 2016

Approval of the thesis:

**RUTHENIUM(0) NANOPARTICLES SUPPORTED ON HAFNIA:
A HIGHLY ACTIVE AND LONG-LIVED CATALYST IN HYDROLYTIC
DEHYDROGENATION OF AMMONIA BORANE**

submitted by **ELİF BETÜL KALKAN** in partial fulfillment of the requirements for
the degree of **Master of Science in Chemistry Department, Middle East
Technical University** by,

Prof. Dr. Gülbin Dural Ünver
Dean, Graduate School of **Natural and Applied Sciences**

Prof. Dr. Cihangir Tanyeli
Head of Department, **Chemistry**

Prof. Dr. Saim Özkar
Supervisor, **Chemistry Dept., METU**

Examining Committee Members:

Prof. Dr. Gülsün Gökağaç
Chemistry Dept., METU

Prof. Dr. Saim Özkâr
Chemistry Dept., METU

Prof. Dr. Ahmet Muhtar Önal
Chemistry Dept., METU

Prof. Dr. İzzet Morkan
Chemistry Dept., Abant İzzet Baysal University

Assoc. Prof. Dr. Emren Nalbant Esentürk
Chemistry Dept., METU

Date: 06/09/2016

I hereby declare that all information in this document has been obtained and presented in accordance with academic rules and ethical conduct. I also declare that, as required by these rules and conduct, I have fully cited and referenced all material and results that are not original to this work.

Name, Last Name: Elif Betül Kalkan

Signature:

ABSTRACT

RUTHENIUM(0) NANOPARTICLES SUPPORTED ON HAFNIA: A HIGHLY ACTIVE AND LONG-LIVED CATALYST IN HYDROLYTIC DEHYDROGENATION OF AMMONIA BORANE

Kalkan, Elif Betül

M. S., Department of Chemistry

Supervisor: Prof. Dr. Saim Özkâr

September 2016, 61 pages

Transition metal(0) nanoparticles are highly active and selective catalyst. When stabilized in organic or aqueous solutions, they can catalyze many reactions. The catalytic activity of metal(0) nanoparticles depends on the particle size and size distribution. However, transition metal(0) nanoparticles have tendency for aggregation to larger particles, ultimately to bulk metal. Metal(0) nanoparticles can be stabilized against aggregation by supporting on the oxide surface. In this project, nanopowder hafnia (HfO_2) was used as support for the stabilization of ruthenium(0) nanoparticles which is found to be one of the most active catalysts in hydrogen release from ammonia borane. Ruthenium(III) cations were impregnated on the surface of HfO_2 and then reduced by sodium borohydride in aqueous solution. Next, ruthenium(0) nanoparticles were used in the catalytic hydrolysis of ammonia borane. Ruthenium(0) nanoparticles supported on hafnia were isolated from the reaction solution by centrifugation and characterized by a combination of advanced analytical techniques including ICP-OES, BET, XRD, SEM, SEM-EDS, TEM, and XPS. Ruthenium(0) nanoparticles supported on hafnia were tested as catalyst in hydrogen generation from the hydrolysis of ammonia borane at ambient temperature. The

kinetics of catalytic hydrolysis were studied depending on the catalyst concentration, metal loading of the support and temperature.

Keywords: Ruthenium(0) nanoparticles; Hydrolysis; Ammonia borane; Heterogeneous catalyst; Hafnia; Hydrogen generation.

ÖZ

HAFNİYA YÜZEYİNDE TUTUNMUŞ RUTENYUM(0) NANOPARÇACIKLARI: OLDUKÇA AKTİF VE UZUN ÖMÜRLÜ KATALİZÖRÜN AMONYAK BORANIN HİDROLİTİK DEHİDROLİZİNDE KULLANILMASI

Kalkan, Elif Betül

Y. Lisans, Kimya Bölümü

Tez Yöneticisi: Prof. Dr. Saim Özkâr

Eylül 2016, 61 sayfa

Geçiş metal nanoparçacıkları, aktifliği ve seçiciliği yüksek katalizörlerdir. Gerek organik fazda ve gerekse sulu çözeltilerde kararlı hale getirilen metal parçacıkları birçok tepkimeyi etkin bir şekilde katalizlemektedir. Metal nanoparçacıklarının katalitik etkinliği tane boyutu ve boyut dağılımı ile yakından ilgilidir. Fakat, geçiş metal nanoparçacıklarının daha büyük parçacıkları ve nihai olarak külçe metali oluşturmak adına toplanma eğilimleri vardır. Metal nanoparçacıkları oksit yüzeyleri desteklenerek toplanmaya karşı kararlı bir hale getirilebilir. Bu projede, amonyak borandan hidrojen salınımı için oldukça aktif katalizörlerden biri olan rutenyum(0) nanoparçacıkları kararlı hale getirebilmek için nanotoz hafniya (HfO_2) ile desteklendirilmiştir. Rutenyum(III) katyonları hafniya yüzeyinde emdirildi ve daha sonra sodium bor hidrür ile indirgendi. Sonrasında, rutenyum(0) nanoparçacıkları amonyak boranın katalitik hidrolizinde kullanıldı. Hafniya ile desteklendirilmiş rutenyum(0) nanoparçacıkları tepkime çözeltisinden santrifüj ile ayrılıp, ICP-OES, BET, XRD, SEM, SEM- EDS, TEM ve XPS gibi gelişmiş analitik yöntemlerinin bir araya gelmesiyle karakterizasyonu yapılmıştır. Hafniya ile desteklendirilmiş rutenyum(0) nanoparçacıkları, amonyak boranın ortam sıcaklığındaki hidrolizinden hidrojen üretilmesinde katalizör olarak denendi. Katalizör derişimi, desteğe yüklenilmiş metal ve sıcaklığa bağlı olarak katalitik hidroliz kinetikleri çalışıldı.

Anahtar Kelimeler: Rutenyum(0) nanoparçacıkları, amonyak boranın hidrolizi, heterojen katalizör, hafniya.

To My Family

ACKNOWLEDGMENT

I would like to express my gratitude to my supervisor Prof. Dr. Saim Özkâr for his valuable support, guidance and encouragement during this study. Without all the assistance and help, this work would have not been accomplished.

My special thanks to Serdar Akbayrak for his endless support to make most of the characterization of the catalysts for this dissertation and other studies during my study.

My friend and laboratory collaborator, Esra Sarica is very appreciated for her support and precious friendship, not only during these studies but also in good times and in bad, in sickness and in health.

Thanks also extended to Prof. Dr. Yalçın Tonbul, Derya Özhava, Seda Tanyıldızı and all other members in ‘Sozkar Research Group’ for their good friendship, scientific collaborations, endless help and motivation.

The last but not the least, my special and sincere thanks go to my whole family and my dear friends for their endless love, invaluable support and considerations in every moment of my life.

TABLE OF CONTENTS

ABSTRACT	v
ÖZ	vii
ACKNOWLEDGMENT	x
TABLE OF CONTENTS	xi
LIST OF TABLES	xiv
LIST OF FIGURES	xv
LI ST OF ABBREVIATIONS	xvii
CHAPTERS	
1. INTRODUCTION	1
1.1. The Hydrogen Issue	1
1.2. Advantages and Disadvantages of Hydrogen Energy	3
1.3. The Hydrogen Economy	5
1.4. Catalytic Hydrolysis of Ammonia Borane for Chemical Hydrogen Storage.....	9
1.5. Transition Metal(0) Nanoclusters.....	11
1.5.1. Fundamental background information	11
1.5.2. Stabilization of nanoclusters against aggregation	12
1.5.3. Full shell (‘magic number’) metal clusters	15
1.5.4. Characterization techniques used in nanocluster chemistry.....	16
1.6. Catalysis	17
1.6.1. General Principles of Catalysis.....	17
1.6.2. Key Definitions in Catalysis	20

1.6.3. Enhancement of Catalytic Activity in Heterogeneous Catalysis by Decreasing the Particle Size.....	20
2. EXPERIMENTAL	23
2.1. Materials	23
2.2. Preparation of ruthenium(0) nanoparticles supported on hafnia (Ru(0)/HfO ₂).....	24
2.3. Characterization of Ruthenium(0) Nanoparticles Supported on Hafnia	25
2.3.1. Inductively Coupled Plasma Optical Emission Spectroscopy (ICP-OES).....	25
2.3.2. Powder X-Ray Diffraction (XRD)	25
2.3.3. Scanning Electron Microscope (SEM) and Electron Diffraction X-Ray.....	25
2.3.4. Transmission Electron Microscope (TEM).....	25
2.3.5. X-Ray Photoelectron Spectroscopy (XPS)	26
2.4. Catalytic hydrolysis of AB using ruthenium(0) nanoparticles supported on hafnia (Ru(0)/HfO ₂).....	26
2.5. Determination of activation energy for hydrolytic dehydrogenation of AB catalyzed by Ru(0)/HfO ₂	28
2.6. Reusability of Ru(0)/HfO ₂ in hydrolysis of AB.....	28
2.7. Determination of the catalytic lifetime of Ru(0)/HfO ₂ in the hydrolysis of AB.....	29
3. RESULTS AND DISCUSSION	31
3.1. Preparation and Characterization of Nanohafnia Supported Ruthenium(0) Nanoparticles	31
3.2. Catalytic Activity of Nanoafnia-stabilized Ruthenium(0) Nanoparticles in Hydrogen Generation from the Hydrolysis of Ammonia Borane	36
3.3. Kinetics of Nanohafnia-stabilized Ruthenium(0) Nanoparticles in Hydrogen Generation from the Hydrolysis of Ammonia Borane	40

3.4. Reusability of Ruthenium(0) Nanoparticles Supported on Hafnia in the Hydrolysis of Ammonia Borane	44
3.5. Catalytic Lifetime of Nanohafnia-stabilized Ruthenium(0) Nanoparticles in Hydrogen Generation from the Hydrolysis of Ammonia Borane	46
4. CONCLUSION	49
REFERENCES.....	51

LIST OF TABLES

TABLES

Table 1. The properties of hydrogen compared to those of other fuels [8].	4
Table 2. Fuel cost comparing between a few hydrogen and gasoline based vehicles.	6
Table 3. The turnover frequency (TOF; $\text{mol H}_2 \cdot (\text{mol Ru})^{-1} (\text{min})^{-1}$), total turnover number (TON; $\text{mol H}_2 \cdot (\text{mol Ru})^{-1}$) and activation energy (E_a ; kJ/mol) values of reported ruthenium catalysts used in hydrogen generation from the hydrolysis of AB.	39

LIST OF FIGURES

FIGURES

Figure 1. Factors supporting and opposing the development of a hydrogen economy [13].	8
Figure 2. Schematic representation of two electrostatically-stabilized nanoparticles [48]. Ions adsorb onto the surface of the nanoparticles by forming an electrical double layer which results in Coulombic repulsion and thus stabilization against aggregation.	13
Figure 3. A) Schematic representation of steric stabilization by adsorption of polymer chains onto a nanoparticle in solution []. The steric layer provided by the adsorbed polymers reveals a large barrier against particle interaction, thus slowing aggregation; B) The inset of the right figure shows a close-up image of two polymer-covered particles interacting. The region between the two particles is crowded since a high local concentration of polymer forms	14
Figure 4. The representation of the relation between the percentage of the surface atoms and number of atoms. Each metal atom has the maximum number of nearest neighbors, which indicates some degree of extra stability to full-shell clusters. Note that the percentage of surface atoms decreases as the number of atoms increases...	15
Figure 5. Common techniques available for the characterization of nanoclusters [73].	16
Figure 6. General kinds of catalysts.	18
Figure 7. Effect of catalyst on the activation energy of the exothermic reaction. A different reaction pathway (shown in red) with a lower activation energy is provided by the presence of the catalyst. The overall thermodynamics and the final result are the same.	19
Figure 8. The experimental setup used in studying the performance of the catalytic hydrolysis of ammonia borane for hydrogen generation rate. 1) Water Bath Circulator, 2) Magnetic Stirrer, 3) Jacketed Schlenk Tube, 4) Water in, 5) Water out, 6) Plastic Hose, 7) Burette Filled with Water []	27
Figure 9. Powder XRD patterns of (a) HfO_2 and (b) Ru^0/HfO_2 (4.0% wt Ru)	32

Figure 10 (a) SEM image and (b) SEM-EDS spectrum of Ru ⁰ /HfO ₂ (4.0% wt. Ru).	33
Figure 11. TEM images of Ru ⁰ /HfO ₂ (4.0% wt. Ru) at different magnifications (a–c) and the corresponding histogram showing the particle size distribution (d).....	35
Figure 12. X-ray photoelectron spectrum of Ru ⁰ /HfO ₂ (4.0% wt. Ru). The inset shows the high resolution scan and deconvolution of Ru 3d bands.....	36
Figure 13. Plot of mol H ₂ /mol H ₃ N•BH ₃ versus time for the hydrolysis of AB (100 mM) starting with Ru ⁰ /HfO ₂ (0.4 mM Ru) with different ruthenium loading at 25.0 ± 0.1°C.	37
Figure 14. (a) The evolution of equivalent hydrogen per mole of AB versus time plot for the hydrolysis of AB starting with Ru ⁰ /HfO ₂ (0.4 mM Ru) and 100 mM AB at various temperatures. (b) The Arrhenius plot for the Ru ⁰ /HfO ₂ in hydrolysis of AB. $\ln k = -7869(1/T) + 28.96$	41
Figure 15. (a) Plots of mol H ₂ /mol H ₃ NBH ₃ versus time depending on the ruthenium concentration in Ru ⁰ /HfO ₂ for the hydrolysis of AB (100 mM) at 25.0 ± 0.1 °C. (b) The logarithmic plot of hydrogen generation rate versus the concentration of Ru; $\ln(\text{rate}) = 0.75 \ln [\text{Ru}] + 3.23$	43
Figure 16. a) Percentage of initial catalytic activity of Ru ⁰ /HfO ₂ ([Ru] = 158 mM) in successive runs after the reuse for the hydrolysis of AB (100 mM) at 25.0 ± 0.1 °C, b) TEM image of Ru ⁰ /HfO ₂ sample harvested after fifth run of hydrolysis of AB. ..	45
Figure 17. a) The variation in turnover number (TON) and turnover frequency (TOF) during the catalytic lifetime experiment performed starting with 3.4 mg Ru ⁰ /HfO ₂ (4.0% wt Ru, and [Ru] = 0.067 mM) in 50 mL solution of AB at 25.0 ± 0.1 °C, b) Catalytic lifetime of reported ruthenium catalysts (TTO = mol H ₂ /mol Ru) in the hydrolysis of AB at room temperature.	47

LIST OF ABBREVIATIONS

AB: Ammonia Borane

AFM: Atomic Force Microscopy

BET: Brunauer Emmet Teller

EDS: Energy Dispersive Spectroscopy

EXAFS: Extended X-Ray Absorption Fine Structure

FC: Fuel Cell

FCEV: Fuel Cell Electric Vehicle

GHG: Greenhouse Gas

HAp: Hydroxylapatite

HPLC: High Performance Liquid Chromatography

ICP-OES: Inductively Coupled Plasma Optical Emission Spectroscopy

IR: Infrared Spectroscopy

MWCNT: Multi-Walled Carbon Nanotube

NIH: National Institutes of Health

NMR: Nuclear Magnetic Resonance Spectroscopy

NP: Nanoparticle

PSSA-co-MA: Poly(4-Styrene Sulfonicacid-Co-Maleic Acid)

P-XRD: Powder X-Ray Diffraction

SEM: Scanning Electron Microscope

SEM/EDS: Scanning Electron Microscope Electron Diffraction X-Ray

STM: Scanning Tunneling Microscopy

TEM: Transmission Electron Microscopy

TOF: Turnover Frequency

TON: Turnover Number

XPS: X-Ray Photoelectron Spectroscopy

X-NW: Xonotlite Nanowire

CHAPTER 1

INTRODUCTION

1.1. The Hydrogen Issue

Energy crisis is among the most important issues which menaced the existence of the man-kind [1]. In retrospect, fossil energy sources could be seen as a good way to overcome world energy problems, but fossil fuels are quite limited to be the principal energy sources because of the quick increase of world energy demand and energy consumption [2]. As global population become to increase from 7 to 9 billion by 2050, world energy consumption is projected to rise with 56% by the next 30 years [3,4]. Fossil fuels are self-produced accumulation of carbon based energy sources as a result of natural processes, which are the dominant source of primary energy in modern economies [5]. The reasons for the extensive use of fossil fuels are that they supply a convenient, storable, transportable, and energy-dense form of chemical energy that can conveniently be turned into thermal energy by way of combustion of the fuels [5]. However, the combustion of fossil fuel leads to formation of greenhouse gas (GHG) emissions and is known as one of the largest sources of GHGs which compose of carbon dioxide (CO₂) mainly [2]. With respect to this, it can be deduced that variances of emissions from fossil fuel combustion have been a major factor affecting total emission trends. The main factors affecting CO₂ emissions contain substitution of natural gas for coal in electricity generation, enhancing in the usage of renewable energy, improvements in vehicle fuel economy, and increase in the efficiencies of appliances and industrial processes [6].

The usage level of distribution of fossil fuel types has evolved substantially during the last 80 years: As a result of advance technologies and world population growth, 80% of the required energy was supplied from coal in 1925 while in the past few decades, 30% came from coal, 45% from petroleum and 25% from natural gas that have a dependency of fossil fuels which will result in out of reserves of fossil fuel eventually to meet energy demand [2]. The experts indicate that reserves are less than 40 years for petroleum, 60 years for natural gas and 250 years for coal [7]. Therefore, the cost of fossil fuel is presumably to rise in the near future. This will put forward renewable energy sources to be drawn on [7]. The inevitable exhaustion of petroleum reserves and other non-renewable energy necessitates the development of new energy sources. As a result of increasing concern about environmental problems, including global warming caused by the emission of gases from the combustion of fossil fuels which is correlated with a number of causalities in warm climate countries, increasing levels of sea water worldwide which threatens seaside cities, and numerous of the natural disasters such as floods, hurricanes, forest fires, and so on, the use of renewable energy sources namely, solar energy, wind power, hydro power, biomass energy, geothermal energy, tidal energy and wave power technologies are sought [8]. Although the renewable energy sources have many good aspects, they have also some disadvantages such as relatively high cost, low efficiency, discontinuity, storage and transportation such as in solar and wind energy which are not always available. Correspondingly, the amount of the loss energy is considerable during storing or moving processes through long distances. Herewith, a necessity of an energy carrier like hydrogen appears as an undeniable fact to overcome these problems.

Recently, the amount of hydrogen produced is about 50 million tons annually worldwide [9] which corresponds to around 2% of the primary energy demand of the world. Mostly, hydrogen is used as a feedstock in the chemical and petrochemical industry in order to produce primarily ammonia and various chemicals which are performed in large quantities and with this purpose, hydrogen production requires big plants. However, quite small amount of hydrogen is reached to end users. Therefore, today hydrogen is still not common as a fuel except for rockets and space shuttles [8].

1.2. Advantages and Disadvantages of Hydrogen Energy

When sustainability and clean energy terms are considered, hydrogen energy has a key role in terms of achieving to utilize non-toxic and renewable energy carrier. In this regard, that 9.5 kg of hydrogen have around same amount energy with 25 kg of gasoline, can be illustrated as an example which shows that hydrogen has a high specific energy on a mass basis (energy/mass) [10,11]. Additionally, hydrogen exists in many production processes including steam reforming of natural gas, gasification of coal, direct and indirect thermochemical decomposition, electrolysis of water and processes ongoing with the presence of direct sunlight and also it can be produced from diverse energy sources involving most renewable ones [11]. Besides, hydrogen can be safely transported via pipelines and used as a chemical feedstock in many synthesis such as polymer, ferrous and non-ferrous metal, petrochemical, food and chemical synthesis, also in metallurgical process industries [11]. Even though when compared to electricity, hydrogen has relatively long periods of time to be stored, there are some difficulties for its storage in liquid form due to requirement of very low temperatures to liquefy hydrogen [11]. Another drawback of utilization of hydrogen as an energy carrier is that although in a combustion, hydrogen generates non-toxic exhaust emissions, excluding some equivalence ratios at high flame temperature which can turn out significant NO_x levels in the exhaust products, hydrogen can burn in lower concentration when contacted with air as a related with safety concerns [11,12,13].

Table 1. The properties of hydrogen compared to those of other fuels [8].

Fuel	Boiling Point [K]	Liquid density [kg m⁻³]	Gas density [kg m⁻³]	Lower heating value (mass) [MJ kg⁻¹]	Lower heating value (liquid) [MJ m⁻³]	Lower flammability limit [vol.%in air]	Upper flammability limit (at 0°C, 1 atm) [vol.% in air]
Hydrogen	20.3	71	0.08	120.0	8960	4	75
Gasoline	350-400	702	4.68	44.4	31170	1	6
Methanol	337	797	-	20.1	16020	7	36
Methane	112	425	0.66	50.0	21250	5	15
Propane	231	507	1.87	46.4	23520	2	10
Ammonia	240	771	0.69	18.6	14350	15	28

Table 1 shows a comparison of hydrogen with hydrocarbon in terms of many aspects. Although hydrogen gas has a poor energy density by volume (2.5 Wh L⁻¹) when compared to hydrocarbons, it has a good energy density by weight (33.3 Wh kg⁻¹). The space requirement for hydrogen is about 3000 times more than for gasoline when an equivalent amount of energy (Table 1) under normal conditions is considered. To enhance the energy density by volume, the gas pressure is increased by paying attention to make the tank not to be lighter, but smaller [8].

1.3. The Hydrogen Economy

The concept of sustainability appeals to a challenge which requires a long-term persistence. Energy is one of the steps of sustainability, which has a great importance when the fact that fossil fuels will not last forever is considered. With this respect, the global energy system with a sustainable path appears as prior concern which addresses the emergence of “hydrogen economy” that is a basically suggested system producing energy by using hydrogen. A hydrogen-based energy system is considered as applicable and consists of many advantages in terms of high-quality and a wide range of applications with an efficient, safe and clean way [14]. The idea behind the hydrogen economy can be summarized simply in four steps: (1) hydrogen is one of the most abundant elements on the Earth; (2) it can be used directly in an internal combustion engine and fuel cell powered cars; (3) heat is produced when molecular hydrogen is combusted with oxygen, and in fact, if this reaction occurs in fuel cell, it generates heat and electricity; (4) when considered emission of CO₂ and production of a variety pollutants, the solely by-product generated by hydrogen is water [9].

Table 2 states that the performance of vehicles with internal combustion engines are absolutely preceded by those powered by fuel cells but, it is forecasted that the almost same energy efficiency is provided by utilizing hydrogen fuel for combustion engines and fuel cells [15]. Experts believe that the total costs of utilizing hydrogen in transportation can be even less than the stated values [1].

Table 2. Fuel cost comparing between a few hydrogen and gasoline based vehicles

Manufacturer	Model	Range with hydrogen fuel (km)	Gasoline consumption (l/100 km) ^a	Hydrogen storage capacity (kg)	Cost of a 100 km journey on gasoline (US\$)	Cost of a 100 km journey on hydrogen (US\$)	Estimated cost of a 100 km journey with locally produced hydrogen (US\$) ^b
BMW	Hydrogen 7 (V12 6.0l ICE)	201	13.9	8	13.43	19.90	13.93
Audi	A2H2	220	5	1.8	4.83	4.09	2.86
Toyota	FCHV bus	690	– ^c	6	–	4.35	3.04
Volkswagen	Touan HyMotion 2004	160	7.2	1.9	6.96	5.94	4.16
Volkswagen	Touan HyMotion 2007	230	6.5	3.2	6.28	6.96	4.87
GM	Hydrogen Minivan	270	–	3.1	–	5.74	4.02
GM	H2H Hummer (V8 ICE)	100	17	5.5	16.42	27.49	19.25
KIA	Borrego FCEV	690	13	7.9	12.56	5.72	4.01
KIA	Sportage	400	8	3.5	7.73	4.37	3.06
Honda	FCX Clarity	430	–	2.7	–	3.14	2.20
Mitsubishi	Lancer Evo IX Hydrogen (Wankel Engine)	110	8.7	2.2	8.40	10.00	7.00
Peugeot	207 Epure (ICE and FC)	350	6.6	3	6.38	4.28	3.00
Mazda	Premacy Hydrogen RE Hybrid	200	11	2.4	10.63	6.00	4.20
Daimler	B-Class F-Cell	400	6	11.1	5.80	13.87	9.71
Mercedes-Benz	F125 Concept	1000	–	7.5	–	3.75	2.62
Hyundai	Tucson FCEV	650	7.5	5.6	7.25	4.31	3.01

ICE, internal combustion engine; FC, fuel cell; FCEV, fuel cell electric vehicle.

^a Based on the same models with gasoline engines or the same vehicles with hybrid fuel consumption.

^b Based on a 30% reduction in the costs of production.

^c No gasoline model has been produced.

Hydrogen markets will strengthen and the basis of it will grow which presents more opportunities for renewable energy systems in the long term. For instance, many renewable energy technologies such as wind turbines or photovoltaics which are transient, will improve electrolysis to produce hydrogen for fuel cells. Hydrogen will be used in the fuel cells to provide electricity by converting chemical energy to compensate high energy demand and to support the transient energy sources [11]. Market access of all these developing technologies to produce, store and use hydrogen will point to the establishment of the hydrogen energy economy, yet there are still some uncertainties related to hydrogen economy which can be summarized as followings [16];

- To produce hydrogen from renewable energy sources is still not economic.
- Hydrogen-powered fuel cells are achievable only if hydrogen is produced in a clean way.
- Transition from hydrocarbons to hydrogen can be achieved in a long term.

In spite of these issues, there is a growing tendency to the hydrogen economy as a result of global environmental problems, technological innovations and supply issues, and, energy security as shown schematically in Fig. 1.

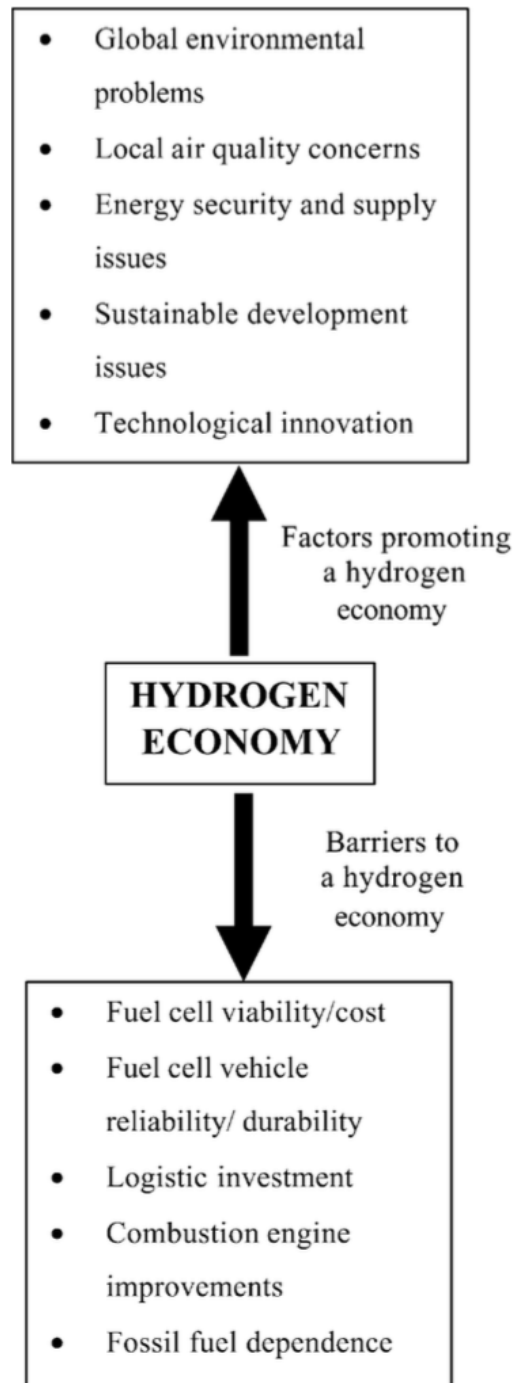


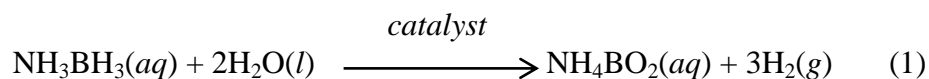
Figure 1. Factors supporting and opposing the development of a hydrogen economy [13].

Hence, in case of replacement of fossil fuels with hydrogen, the energy issue and many of environmental problems could be solved; however, molecular hydrogen is not available on the Earth, which means molecular hydrogen has to be obtained from hydrogen-rich compounds by using energy, and this is the reason why hydrogen energy is pronounced as an energy carrier instead of an alternative fuel [17,18]. This is the one of the major problems of standing behind the hydrogen economy. In this regard, chemical hydrogen storage has great importance in the sense of high hydrogen content.

1.4. Catalytic Hydrolysis of Ammonia Borane for Chemical Hydrogen Storage

For hydrogen sources to be used in fuel cells, chemical storage materials are quite rewarding when considering high hydrogen contents. Boron- or nitrogen-based compounds (Li/NaBH_4 , N_2H_4 and $\text{LiNH}_2\text{--LiH}$ etc.) have drawn more attention among all [19,20,21,22,23].

Boron hydrides were investigated as hydrogen storage chemical materials by considering their comparatively high gravimetric and volumetric hydrogen density [24,25]. The simplest B-N compound ammonia borane (NH_3BH_3 , AB) is known to be the most promising hydrogen storage material among boron hydrides for settled hydrogen storage applications on the account of its low molecular weight (30.9 g mol^{-1}) and a hydrogen capacity as high as 19.6 wt.%, surpassing those of gasoline and Li/NaBH_4 [18,26]. Hydrogen stored in the AB complex can be released by either thermolysis [27] or solvolysis [28] in the presence of suitable catalyst. Since high temperature is required for the thermolysis [29], the latter reaction is highly advantageous for hydrogen generation from AB. Hydrolysis of AB has been regarded as an efficient approach because of its rapid hydrogen release in the presence of a suitable catalyst (eq.1) [30].



The idea of hydrolysis of ammonia borane in the presence of supported transition metals was applied first time by Chandra and Xu in 2006 [31]. Their studies have shown that when suitable metal catalyst is added into ammonia borane solution in catalytic amount, it releases stoichiometric amount of H_2 from aqueous NH_3BH_3 mole ratio up to 3.0. They studied on both non-noble and noble metal catalysts. For non-noble metal catalysts, Co, Cu, Fe, which were supported on $\gamma-Al_2O_3$, SiO_2 and C, Co/C showed highest activity among them except for Fe which showed no activity during hydrolysis reaction [32]; however, hydrogen generation from hydrolytic dehydrogenation of ammonia borane was found to be faster in the presence of noble metal catalyst, Rh, Ru, Pt at room temperature where the highest activity belongs to Pt/C 20 wt.% [33]. At this respect, it can be said that noble metal catalysts are more reactive and selective and require less severe reaction conditions. Even if they are more expensive than non-noble transition metals, the spent catalyst can be recovered and the precious metal reprocessed into the fresh catalysts.

Ruthenium is one of the most active catalysts in hydrogen generation from the hydrolysis of AB under mild conditions. Although there exist a wealth of reports on the hydrogenation of AB using ruthenium catalysts such as Ru^0/CeO_2 [83], $Ru(0)/MWCNT$ [84], $Ru(0)/TiO_2$ [87], $Ru/nanodiamond$ [89], $Ru(0)/PSSA-co-MA$ [91], $Ru(0)/HAp$ [94] and $Ru/X-NW$ [95], there is no example of ruthenium catalyst with long lifetime for the hydrogen release from ammonia borane. Therefore, ruthenium gains importance in terms of high activity and stability when supported on a suitable material for the hydrolysis of AB. Activity and stability of metal nanoparticles catalysts can be improved by using suitable supporting materials in order to avoid the tendency toward the aggregation of nanoparticles which cause a reduction in catalytic activity [34], such as graphene [35], carbon nanotube [36], carbon black [37], zeolites [38], alumina (Al_2O_3) [39], ceria (CeO_2) [40,41], titania (TiO_2) [42], and zirconia (ZrO_2) [43].

Among metal oxides of Group 4 (TiO_2 , ZrO_2 , HfO_2) in the periodic table, hafnium dioxide (HfO_2 , hafnia) is widely used in electronic field due to its quite high dielectric constant, making it a suitable alternative to silicon dioxide insulating layers for the improvement of integrated circuits [44,45]. Hafnia has also high chemical and

thermal stability [46,47], which makes it an alternative supporting material for metal nanoparticles used in catalysis.

Herein, we present the synthesis and characterization of ruthenium(0) nanoparticles supported on hafnia (HfO_2) as a catalyst in hydrogen generation from hydrolysis of ammonia borane. The ruthenium(0) nanoparticles supported on hafnia were characterized by ICP-OES, BET, XRD, SEM, SEM-EDS, TEM, and XPS. The results reveal the formation of well-dispersed ruthenium(0) nanoparticles on the surface of hafnia nanopowder. The resulting ruthenium(0) nanoparticles were found to be highly active and long-lived catalyst in hydrogen generation from the hydrolysis of ammonia borane at room temperature. The kinetics of the catalytic hydrolysis of ammonia borane was studied depending on the catalyst concentration, metal loading of the support and the temperature. The rate law of the catalytic reaction was established. The activation energy and activation parameters of catalytic hydrolysis reaction were acquired through a kinetic study of the hydrolysis of ammonia borane catalyzed by ruthenium(0) nanoparticles supported on hafnia.

1.5. Transition Metal(0) Nanoclusters

1.5.1. Fundamental background information

Nanoclusters which are defined as near-monodispersed particles with the size of less than 10 nm (100 Å) in diameter [48] have drawn great attraction for a long time. The main reasons for that, firstly, the properties of these particles stand somewhere between those of bulk and single-particle species [49,50], which supports the belief of the future unique properties of nanoclusters. The uses of nanoclusters include photochemical pattern applications such as flat-panel displays [51], quantum dots [52] or quantum computers [53] and devices [54,55], industrial lithography [56], chemical sensors [57], ‘ferrofluids’ for cell separations [58] and light-emitting diodes [59], which can be shown as examples of magnificent potential uses. In addition, these ‘strange morsels of matter’ [60] have a considerable potential in the sense of new types of higher activity and selectivity. To illustrate, the significant work of

Schmid's laboratories gets a glimpse of such unexpected catalytic selectivities that are anticipated properties of nanoclusters [61].

There are two basic reasons for why chemists believe that nanoclusters have great potential to be more active and selective as catalysts rather than those of today; first of all, a major percentage of metal nanocluster atoms lie on the surface, and the atoms on surface are not ordered as in the same way like those in the bulk [60]. Moreover, the electrons in a nanocluster are confined to spaces to restrict their motions in specific energy levels that can be as small as a few atom-widths across, giving rise to quantum size effects [60]. Finally, the possibility of controlling both surface ligands and nanocluster size in a modifiable, quantitative and articulable way for supported heterogeneous catalysts is offered by nanoclusters [62].

1.5.2. Stabilization of nanoclusters against aggregation

Nanoclusters are needed to be stabilized against aggregation into larger particles and ultimately, bulk material because they are stable only kinetically. Thermodynamically, their stability is minimum. Stabilization can be achieved in two common ways: electrostatic (charge, or 'inorganic') stabilization and steric ('organic') stabilization [62].

Electrostatic stabilization takes place by means of the adsorption of ions to the often electrophilic metal surface [63]. With this adsorption, an electrical double (really multi-) layer is created [64], which is concluded with a Coulombic repulsion force between individual particles, Fig. 2.

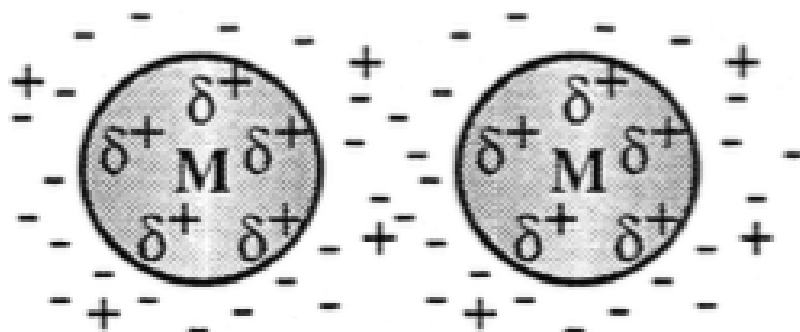


Figure 2. Schematic representation of two electrostatically-stabilized nanoparticles [48]. Ions adsorb onto the surface of the nanoparticles by forming an electrical double layer which results in Coulombic repulsion and thus stabilization against aggregation.

Steric stabilization is accomplished by preventing colloidal particles from aggregating with the help of surrounding the metal center by layers of material that are sterically bulky [63], such as polymers [65], ligands [66] or surfactants [67]. A steric barrier which is created by these large adsorbates, prevents close contact of the metal particle centers, Fig. 3.

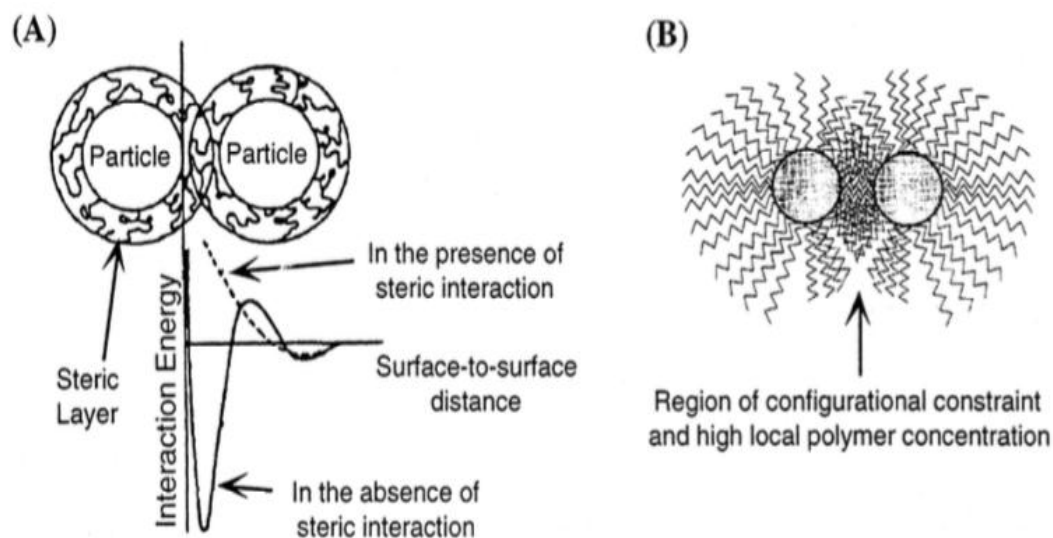


Figure 3. A) Schematic representation of steric stabilization by adsorption of polymer chains onto a nanoparticle in solution [68]. The steric layer provided by the adsorbed polymers reveals a large barrier against particle interaction, thus slowing aggregation; B) The inset of the right figure shows a close-up image of two polymer-covered particles interacting. The region between the two particles is crowded since a high local concentration of polymer forms [69].

Polymers are one of the most used protectants over nanoclusters in order to coordinate to the particle surface to function effectively. The suitable polymer is chosen by considering the solubility of the solvent of choice, the metal colloid precursor, , and the stabilizing ability of the polymer for the reduced metal particles in the colloidal state [66].

1.5.3. Full shell ('magic number') metal clusters

Figure 4 represents metal clusters with a complete, regular outer geometry are designated full-shell, or 'magic number', clusters. The term 'magic number' is controversial and probably somewhat misleading. A more appropriate term for these clusters may be "full-shell" clusters, that is, clusters which have some extra stability partially simply because of their close-packed, full-shell nature [70].

Full-shell clusters are built up around a single metal atom by successively packing shells of metal atoms. The equation, $y = 10n^2 + 2$ ($n > 0$) gives the total number of metal atoms, y , per n th shell [71]. Therefore, full-shell metal clusters include M_{13} ($1 + 12 = 13$), M_{55} ($13 + 42 = 55$), M_{147} ($55 + 92 = 147$), M_{309} , M_{561} , M_{923} (and so on) metal atoms [62].






Full-Shell "Magic Number" Clusters					
Number of shells	1	2	3	4	5
Number of atoms in cluster	M_{13}	M_{55}	M_{147}	M_{309}	M_{561}
Percentage surface atoms	92%	76%	63%	52%	45%

Figure 4. The representation of the relation between the percentage of the surface atoms and number of atoms. Each metal atom has the maximum number of nearest neighbors, which indicates some degree of extra stability to full-shell clusters. Note that the percentage of surface atoms decreases as the number of atoms increases.

Many nanocluster distributions occur center around one of these full-shell geometries. Unsurprisingly, it is believed that full-shell clusters have brought stability since their densely-packed structures supplies the maximum number of metal–metal bonds [72].

1.5.4. Characterization techniques used in nanocluster chemistry

The main aim of nanocluster characterization is to determine particle size and overall composition. In addition, surface composition is investigated, which is a more compelling task. Figure 5 represents a good overall scheme of the techniques mostly used to characterize nanoclusters [73].

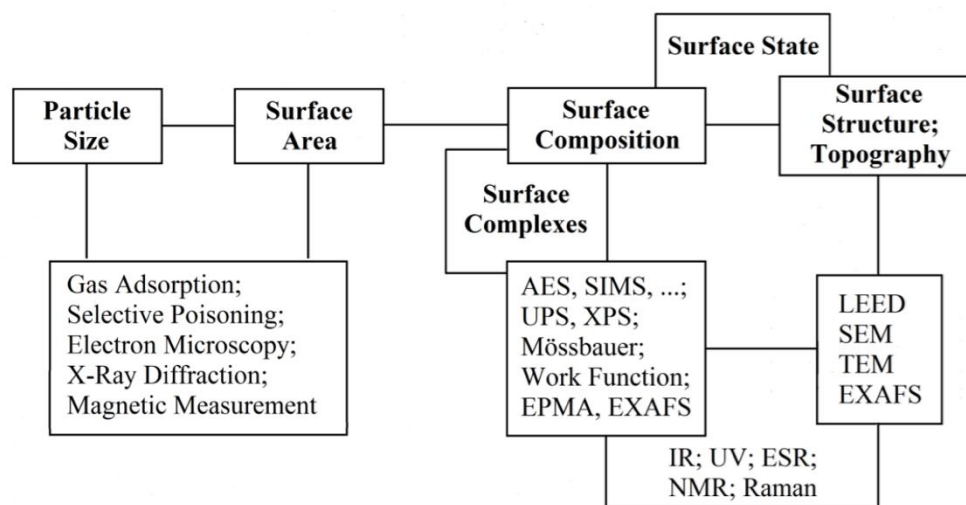


Figure 5. Common techniques available for the characterization of nanoclusters [73].

Transmission electron microscopy (TEM), nuclear magnetic resonance spectroscopy (NMR), UV–Visible spectroscopy (UV–Vis), elemental analysis, infrared spectroscopy (IR), and energy dispersive spectroscopy (EDS) are some of the characterization techniques used in establishing structural, compositional and

topographic characterization of nanoclusters. To be more comprehensive, the following methods are also used: scanning tunneling microscopy (STM), analytical ultracentrifugation–sedimentation, atomic force microscopy (AFM), high performance liquid chromatography (HPLC), light scattering, extended X-ray absorption fine structure (EXAFS), time-of-flight mass spectrometry, ion-exchange chromatography or electrophoresis and magnetic susceptibility. Since nanoclusters usually do not crystallize, X-ray crystallography is not a suitable technique for characterizing such molecules. When definition of the related colloid state is considered, obviously, it can be seen that it is a state that cannot be crystallized [62].

1.6. Catalysis

1.6.1. General Principles of Catalysis

A catalyst is a substance that enhances the rate of a chemical reaction with the absence of being changed during the process, which means a catalyst remains same after the reaction as before. The occurrence of the increase in the rate of a chemical reaction as a result of the participation of a catalyst is called as catalysis. Since the catalyst is not consumed stoichiometrically in the process, each catalyst molecule can be used in over many cycles; therefore, only a small amount of catalyst relative to substrate is needed. There are many kinds of catalysts including the proton and many different types of chemical compounds such as organometallic complexes, Lewis acids, enzymes, organic or inorganic polymers, and so on. However, simply, it can be said that mainly, there are three types of catalysis; (i) heterogeneous catalysis, (ii) homogeneous catalysis, and (iii) biocatalysis as shown in Figure 6 [74].

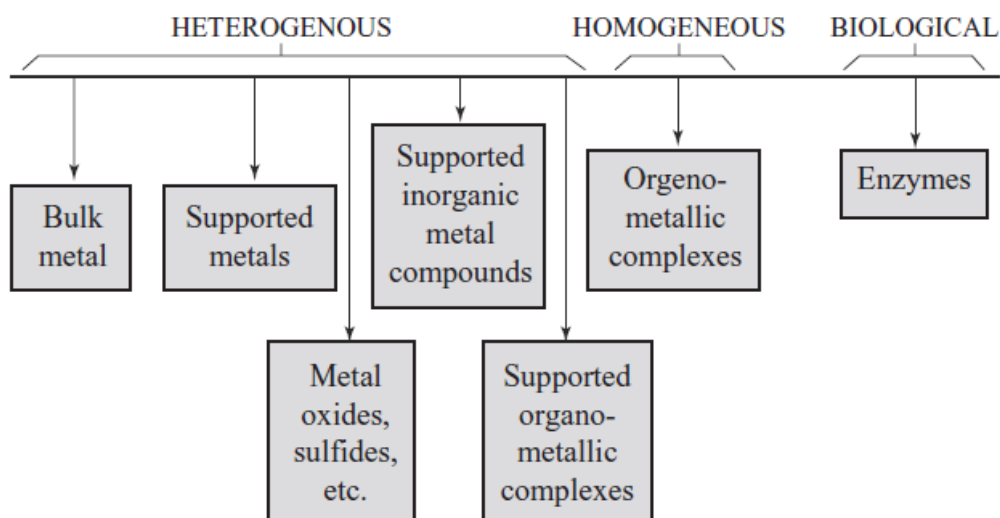


Figure 6. General kinds of catalysts.

Mainly, the classification of heterogeneous and homogeneous catalysis is based on whether the catalyst is in the different phase with the substrate or not. If the difference in the phases does not exist between the catalyst and the reactants -also products-, then it is called as homogeneous catalyst. Most of the homogeneous catalysts are comprised of transition metal atom which is stabilized by a ligand. The ligands can usually be defined as organic molecules that bind to the metal atom to form coordination complex. Correspondingly, the characteristics of a homogeneous catalyst can be varied by changing the kind of ligand.

Heterogeneous catalysts refer where the phase of catalyst are different from the phase of reactant. In heterogeneous catalysis, diffusion of the reactants occur through the catalyst surface (usually metal surface) and adsorb onto it, and in the meantime, chemical bonds start to form. After reaction, the products diffuse away from the surface.

The idea behind to increase the rate of reaction with a catalyst is based on transition state theory which explains the reaction rates of elementary chemical reactions. Catalysis provides an alternative mechanism which consists of lower activation energy and a different transition state. In the transition-state theory, since transition

state is retained on the surface of catalyst resulting with loss of translational freedom, the activation entropy of a catalyzed reaction will usually be lower as compared to uncatalyzed chemical reaction. As it is expected, there must be a corresponding decrease in the activation enthalpy to compensate this decrease. Therefore, the activation energy of a catalyzed reaction should be less than the corresponding uncatalyzed reaction in pursuance of theory (Figure 7).

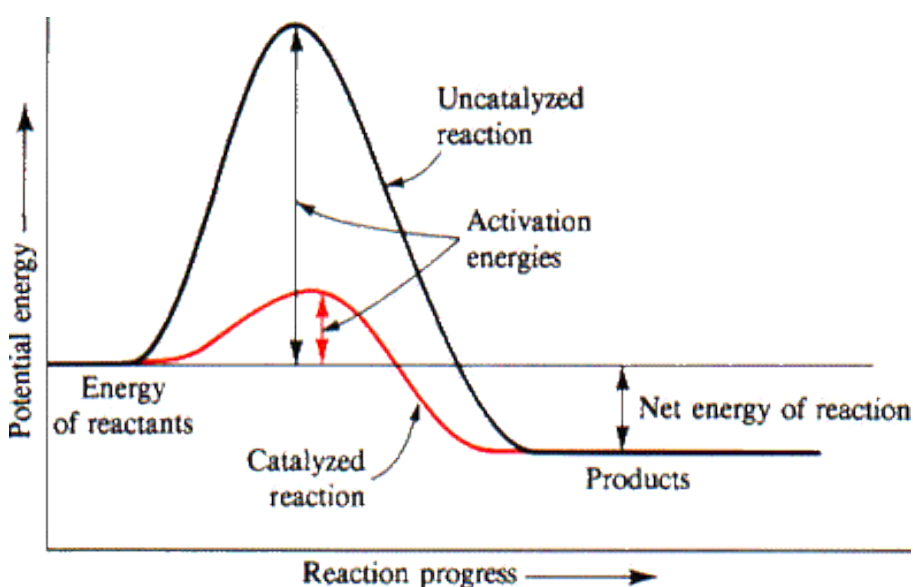


Figure 7. Effect of catalyst on the activation energy of the exothermic reaction. A different reaction pathway (shown in red) with a lower activation energy is provided by the presence of the catalyst. The overall thermodynamics and the final result are the same.

Eventually, the energy necessary to reach the transition state is present via more molecular collisions. Therefore, catalysts can provide reactions which or else would be blocked or slowed by a kinetic barrier. When the activity of a catalyst can be expressed by the turnover frequency (TOF), the catalytic efficiency can be identified by the turnover number (or TON).

1.6.2. Key Definitions in Catalysis

The turnover frequency TOF quantifies the specific activity of a catalyst for a special reaction under defined reaction conditions by the number of catalytic cycles occurring per unit time.

$$TOF (t^{-1}) = \frac{Mol\ of\ Product}{Mol\ of\ Catalyst} \times \frac{1}{t} \quad (2)$$

The catalytic lifetime of a catalyst is generally described as total turnover number (TON) that specifies the number of moles of product per mole of catalyst Eq. (3); this number specifies the maximum use that can be made of a catalyst for a special reaction under defined conditions by a number of molecular reactions or reaction cycles.

$$TON = \frac{Mol\ of\ Product}{Mol\ of\ Catalyst} \quad (3)$$

The relation between TOF and TON can be expressed as following;

$$TON = TOF [time^{-1}] * lifetime\ of\ the\ catalyst [time]$$

1.6.3. Enhancement of Catalytic Activity in Heterogeneous Catalysis by Decreasing the Particle Size

The local size of catalyst particles affects their performance (i.e., activity and selectivity) and to see how advances in nanoscience have contributed to a detailed understanding of the effects of particle size on catalyst performance as proceeding to nanoscale, a significant change in the intrinsic properties of materials can be taken into consideration. The enhancing activity of the heterogeneous catalyst by the decrease of particle size is one of the examples for these changes in sense the activity of heterogeneous catalysts is directly related to surface area [75]. Specially, metal

nanoclusters gain a new perspective in terms of surface chemistry because they provide unusual surface morphologies and have more reactive surfaces. Consequently, they created a major potential for catalysis due to their large surface area. When the ultimate large surface areas of them are considered, many of the lying atoms on the surface provides a good atom economy in surface-liquid, surface-gas, or even surface-solid reactions [76].

CHAPTER 2

EXPERIMENTAL

2.1. Materials

Ruthenium(III) chloride trihydrate ($\text{RuCl}_3 \cdot 3\text{H}_2\text{O}$), hafnia (HfO_2 , particle size ≈ 100 nm), and ammonia-borane (AB, 97%) were purchased from Aldrich. Sodium borohydride (NaBH_4 , 98%) was purchased from Merck. Deionized water was distilled by water purification system (Milli-Q System). All glassware and Teflon-coated magnetic stir bars were cleaned with acetone, followed by copious rinsing with distilled water before drying in an oven at 150 °C.

2.2. Preparation of ruthenium(0) nanoparticles supported on hafnia (Ru(0)/HfO₂)

HfO₂ (400 mg) was added into 50 mL H₂O in a 100 mL beaker, and ultrasonication was applied for 10 min. Then, required quantity of RuCl₃·3H₂O (46.2 mg) was added in this slurry, and again ultrasonication was applied for 20 min to deagglomerate and disperse the particles into liquid media. This slurry was stirred at room temperature for 24 h and then 10 mL of 177 mM NaBH₄ solution was added into Ru³⁺/HfO₂ sample dropwise by Pasteur pipette. When the hydrogen generation from the reaction solution ended (~1 h), Ru(0)/HfO₂ sample were isolated by centrifugation and washed five times with 50 mL of deionized water to remove metaborate anions and dried under vacuum (10⁻³ torr) at 60 °C for 12 h. The samples of Ru(0)/HfO₂ were bottled as grey powders. Ruthenium content of the Ru(0)/HfO₂ sample was found to be 4.0 wt.% by ICP-OES analysis.

2.3. Characterization of Ruthenium(0) Nanoparticles Supported on Hafnia

2.3.1. Inductively Coupled Plasma Optical Emission Spectroscopy (ICP-OES)

The ruthenium content of the Ru⁰/HfO₂ sample was determined by Inductively Coupled Plasma Optical Emission Spectroscopy (ICP-OES, Leeman-Direct Reading Echelle) after the sample was completely dissolved in the mixture of HNO₃/HCl (1/3 ratio).

2.3.2. Powder X-Ray Diffraction (XRD)

X-Ray Diffraction pattern of the samples were characterized by a Rigaku Mini-Flex X-ray powder Diffractometer (XRD) with a radiation source of Cu-K α line ($\lambda=1,54056$ Å) with the scanning rate within a 2θ range of 3 to 90° is 2 °/min.

2.3.3. Scanning Electron Microscope (SEM) and Electron Diffraction X-Ray

Scanning electron microscope (SEM) images were taken using a JEOL JSM-5310LV at 15 kV and 33 Pa in a high-vacuum mode without metal coating on carbon support.

2.3.4. Transmission Electron Microscope (TEM)

Transmission electron microscopy (TEM) was performed on a JEM-2100F (JEOL) microscope operating at 200 kV. A small amount of powder sample was placed on the holey carbon grid of the transmission electron microscope. Samples were examined at magnification between 500 and 700 K.

2.3.5. X-Ray Photoelectron Spectroscopy (XPS)

The X-ray photoelectron spectroscopy (XPS) analysis was performed on a Physical Electronics 5800 spectrometer equipped with a hemispherical analyzer and using monochromatic Al K α radiation of 1486.6 eV, the X-ray tube working at 15 kV, 350 W and pass energy of 23.5 keV.

2.4. Catalytic hydrolysis of AB using ruthenium(0) nanoparticles supported on hafnia (Ru(0)/HfO₂)

Ruthenium(0) nanoparticles supported on hafnia (Ru⁰/HfO₂) were used as catalysts for the catalytic hydrolysis of AB. Before starting the catalytic hydrolysis of AB, a jacketed reaction flask (20 mL) containing a Teflon-coated stir bar was placed on a magnetic stirrer (Heidolph MR-301) and thermostated to 25.0 ± 0.1 °C by circulating water through its jacket from a constant temperature bath. Then, a graduated glass tube (60 cm in height and 3.0 cm in diameter) filled with water was connected to the reaction flask to measure the volume of the hydrogen gas to be evolved from the reaction. Next, 10 mg powder of Ru⁰/HfO₂ (4.0 wt.% Ru) was dispersed in 10 mL distilled water in the reaction flask thermostated at 25.0 ± 0.1 °C. Then, 31.8 mg AB (1.0 mmol H₃N.BH₃) was added into the flask and the reaction medium was stirred at 1000 rpm. After adding ammonia borane, the catalytic hydrolysis of AB started immediately. The volume of hydrogen gas evolved was measured by recording the displacement of water level every 30 s at constant atmospheric pressure of 693 Torr. The reaction was stopped when no more hydrogen evolution was observed.

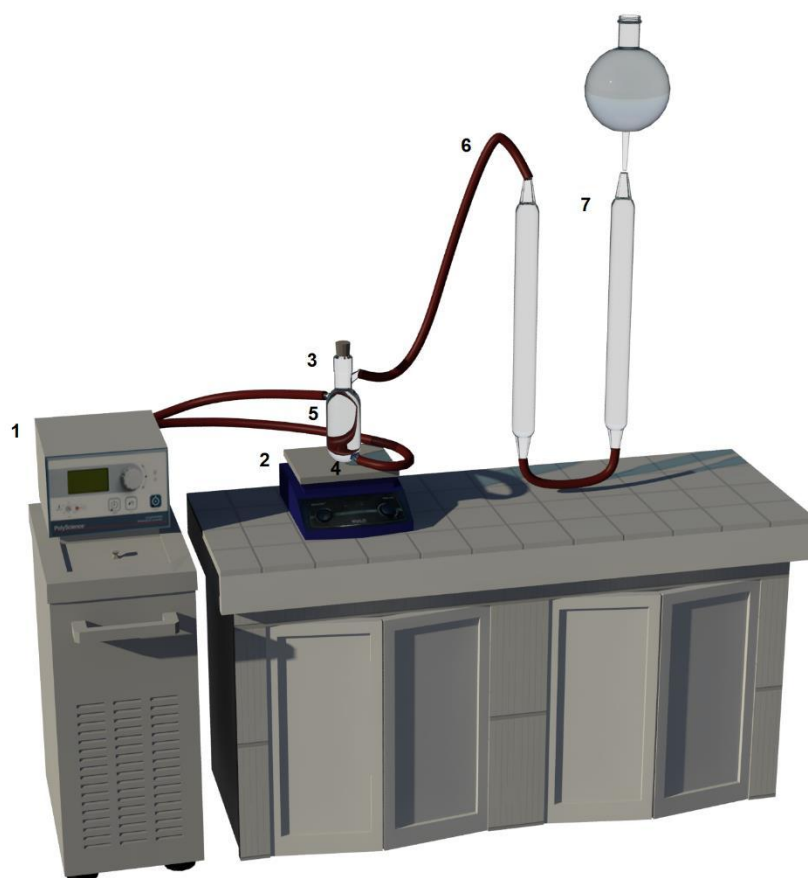


Figure 8. The experimental setup used in studying the performance of the catalytic hydrolysis of ammonia borane for hydrogen generation rate. 1) Water Bath Circulator, 2) Magnetic Stirrer, 3) Jacketed Schlenk Tube, 4) Water in, 5) Water out, 6) Plastic Hose, 7) Burette Filled with Water [77].

2.5. Determination of activation energy for hydrolytic dehydrogenation of AB catalyzed by Ru(0)/HfO₂

In a typical experiment, catalytic hydrolysis of NH₃BH₃ using ruthenium(0) nanoparticles supported on hafnia was performed as two different sets of experiment in order to obtain the activation energy. In the first set, the hydrolysis reaction was performed starting with different initial concentration of ruthenium(0) (0.10, 0.20, 0.40, 0.80 mM) at room temperature (25.0 ± 0.1 °C) while the initial ammonia borane concentration was kept constant at 100 mM (31.8 mg = 1.00 mmol). The second set of experiments were performed in the presence of ruthenium(0)nanoparticles at constant catalyst (4% wt. ruthenium [Ru] = 0.40 mM) and substrate (100 mM) concentrations and at various temperatures (25, 30, 35, 40 °C) in order to obtain the activation energy (E_a).

2.6. Reusability of Ru(0)/HfO₂ in hydrolysis of AB

After the complete hydrolysis of AB started with 10 mL of 100 mM AB (31.8 mg H₃NBH₃), and 40 mg Ru(0)/HfO₂ (4.0 % wt. ruthenium, [Ru] = 0.4 mM) at 25 ± 0.1 °C, the catalyst was isolated as a powder by centrifugation and dried under vacuum (10⁻³ torr) at 60 °C after washing with 50 mL of water. The isolated samples of Ru⁰/HfO₂ were weighed and redispersed in 10 mL solution of 100 mM AB for a subsequent run of hydrolysis which was then started immediately and continued until the completion of hydrogen evolution at 25.0 ± 0.1 °C. This hydrogen generation process was repeated 5 times in the same way at 25 ± 0.1 °C.

2.7.Determination of the catalytic lifetime of Ru(0)/HfO₂ in the hydrolysis of AB

The catalytic lifetime of Ru(0)/HfO₂ in the hydrolysis of AB was determined by measuring the total turnover number (TON). Such a lifetime experiment was started with a 50 mL solution containing 3.4 mg of Ru⁰/HfO₂ (ruthenium loading = 4.0% wt. Ru, and [Ru] = 0.067 mM) and AB at 25.0 ± 0.1 °C. When all the ammonia-borane present in the solution was completely hydrolyzed, more AB was added and the reaction was continued in this way until no hydrogen gas evolution was observed.

CHAPTER 3

RESULTS AND DISCUSSION

3.1. Preparation and Characterization of Nanohafnia Supported Ruthenium(0) Nanoparticles

Ruthenium(0) nanoparticles supported on nanohafnia (Ru^0/HfO_2) were prepared by a simple method. First, ruthenium(III) ions were impregnated on nanohafnia from the aqueous solution of ruthenium(III) chloride and then reduced in aqueous medium by sodium borohydride at room temperature. Ru^0/HfO_2 was isolated from the reaction solution by centrifugation, copious washing with water, and drying under vacuum (10^{-3} Torr) at 60 °C and characterized by ICP-OES, BET, XRD, SEM, SEM-EDS, TEM and XPS.

The BET nitrogen adsorption-desorption analysis gave the surface area of hafnia and Ru^0/HfO_2 (4.0% wt. Ru) as 6.1 m²/g and 15.8 m²/g, respectively. The increase in the surface area of hafnia upon ruthenium loading implies the existence of ruthenium nanoparticles on the surface of nanohafnia.

The powder XRD patterns of hafnia nanopowders and Ru^0/HfO_2 with a 4.0% wt. ruthenium loading (Fig. 9) exhibits peaks at 24.18, 28.33, 31.66, 34.35, 35.53, 49.55, 50.43, 55.71, 60.15, and 66.12° assigned to the (110), (-111), (111), (200), (002), (220), (022), (310), (131), and (023) reflections of HfO_2 , respectively (JPDS = 34-0104). No change is observable in intensity and position of the characteristic diffraction peaks of hafnia upon loading the ruthenium nanoparticles. This observation indicates that after reduction of ruthenium(III) ions, hafnia remains intact and there is no noticeable alteration in the framework lattice or loss in the

crystallinity of host material. There is no observable peak attributable to ruthenium nanoparticles in Fig. 9b, most likely as a result of low ruthenium loading on hafnia.

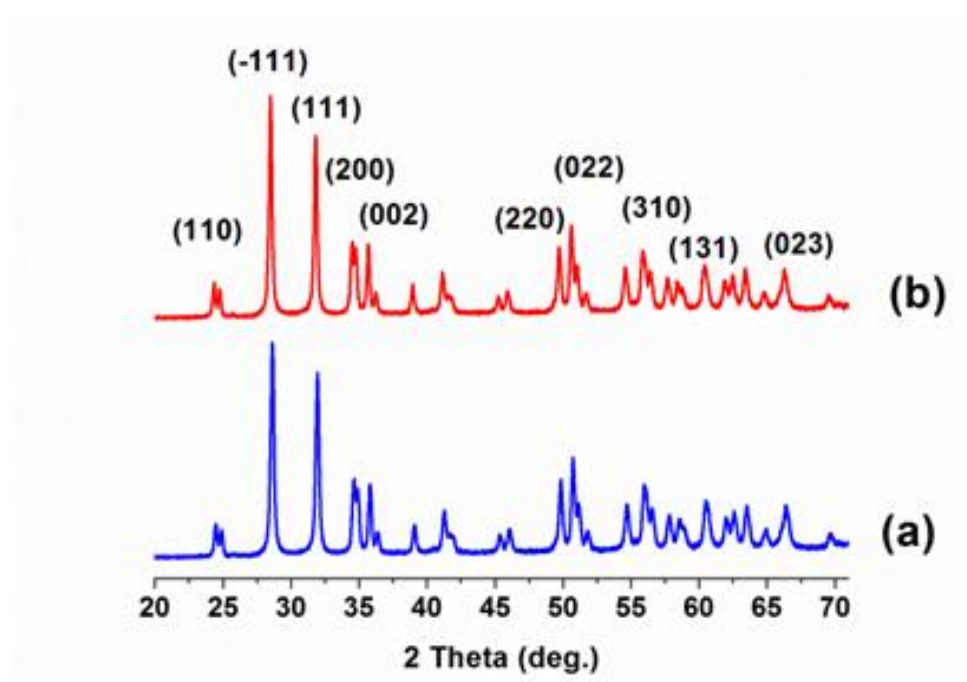


Figure 9. Powder XRD patterns of (a) HfO_2 and (b) Ru^0/HfO_2 (4.0% wt Ru)

Figure 10 exhibits the SEM image and SEM-EDS spectrum of Ru^0/HfO_2 . While SEM image (Fig. 10(a)) shows that no bulk ruthenium was formed, SEM-EDS (Fig. 10 (b)) indicates that ruthenium is the only element detected in the sample in addition to the framework elements of hafnia (Hf, O).

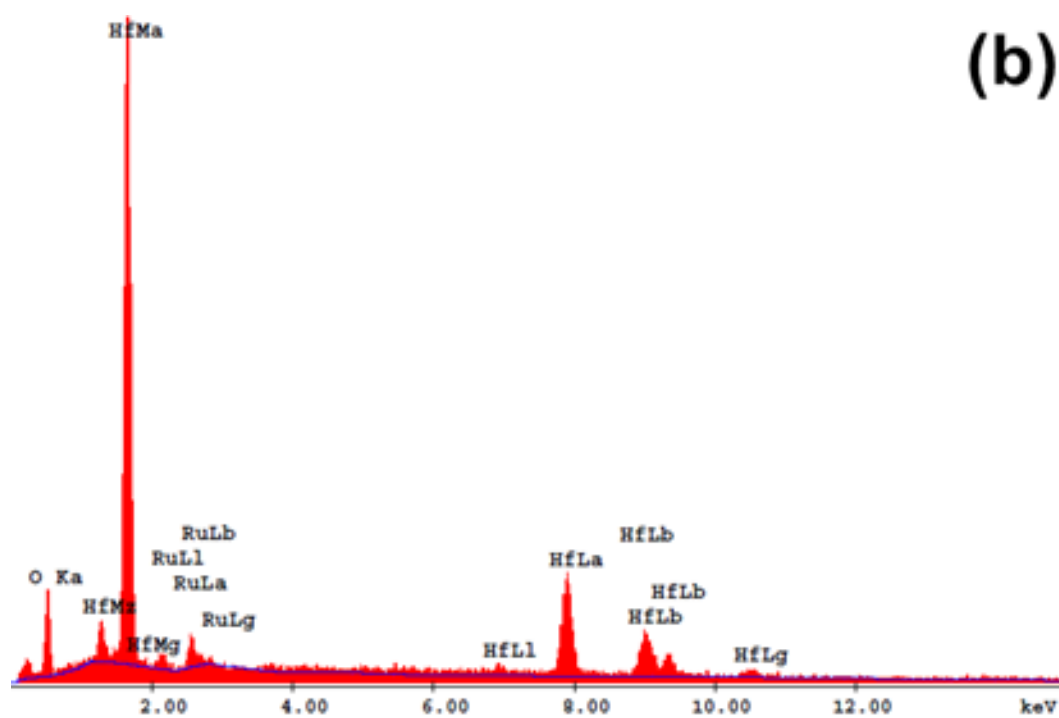
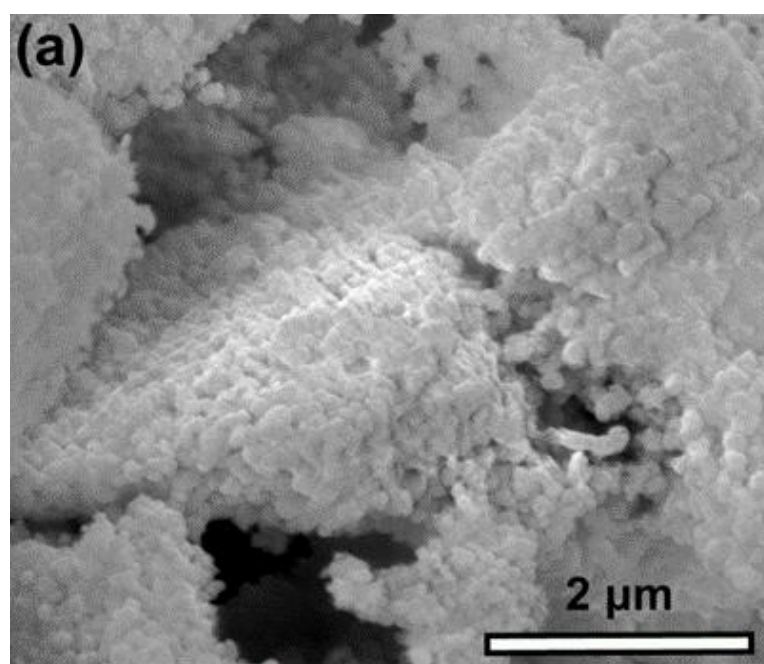


Figure 10. (a) SEM image and (b) SEM-EDS spectrum of Ru^0/HfO_2 (4.0% wt. Ru).

The morphology and size of ruthenium(0) nanoparticles supported on the surface of nanohafnia were investigated by high resolution TEM (Fig. 11a–c). One can see the ruthenium(0) nanoparticles with particle size in the range 2.4–5.0 nm dispersed on the surface of nanohafnia. The average diameter of ruthenium(0) nanoparticles is 3.5 ± 0.6 nm as shown in the histogram given in Fig. 11d). As clearly seen from the TEM images and the increase in BET surface area of Ru^0/HfO_2 as compared to HfO_2 , hafnia provides a large fraction of catalytically active surface sites for the ruthenium(0) nanoparticles which have little depth on hafnia surface. In other words, ruthenium(0) nanoparticles do not intrude into the surface of nanohafnia framework.

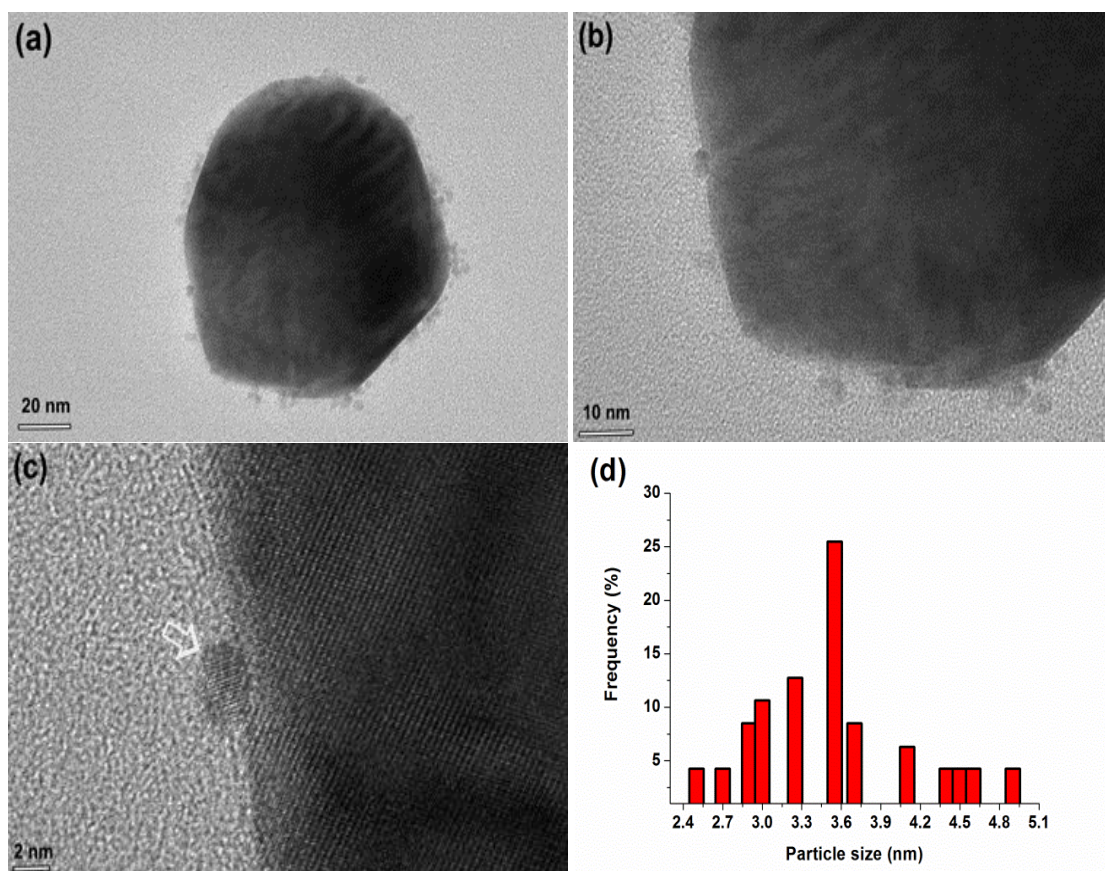


Figure 11. TEM images of Ru⁰/HfO₂ (4.0% wt. Ru) at different magnifications (a–c) and the corresponding histogram showing the particle size distribution (d).

The composition of Ru⁰/HfO₂ and the oxidation state of ruthenium were also studied by XPS technique. The survey-scan XPS spectrum of Ru⁰/HfO₂ sample with 4.0% wt. Ru loading in Fig. 12 shows the presence of all the elements Ru, Hf, and O in agreement with the SEM-EDS result. The inset of Fig. 12 shows the high resolution XPS of Ru⁰/HfO₂ sample with 4.0% wt. Ru loading. Since the Ru(0) 3d_{3/2} peak overlaps with the C 1s peak at 282.83 eV only the peak at 279.06 eV can be assigned to Ru⁰ 3d_{5/2} with certainty by comparing to the values of metallic ruthenium [78,79].

The band at 286.07 eV might be attributed to ruthenium oxide [80], which might be formed during the XPS sampling.

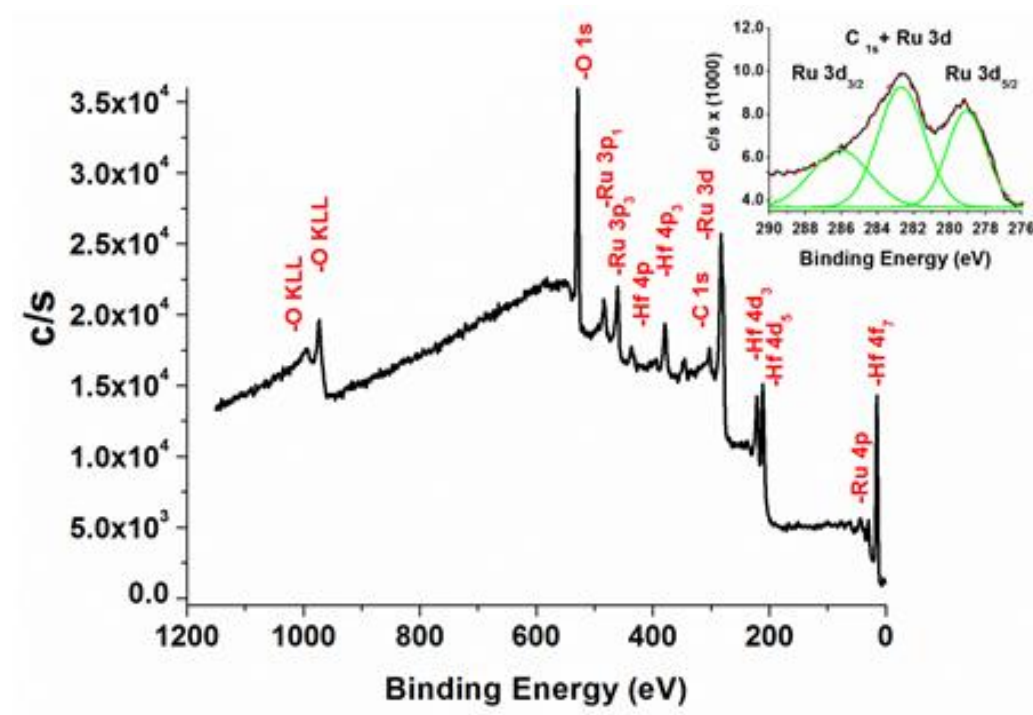


Figure 12. X-ray photoelectron spectrum of Ru⁰/HfO₂ (4.0% wt. Ru). The inset shows the high resolution scan and deconvolution of Ru 3d bands.

3.2. Catalytic Activity of Nanohafnia-stabilized Ruthenium(0) Nanoparticles in Hydrogen Generation from the Hydrolysis of Ammonia Borane

The hafnia-supported ruthenium(0) nanoparticles were tested for their catalytic activity in hydrogen generation from the hydrolysis of ammonia borane. The catalytic hydrolysis of ammonia borane was followed by monitoring the change in H₂ volume, which was then converted into the equivalent H₂ per mole of ammonia borane using the known 3:1 H₂/AB stoichiometry (Eq. 1). Before starting the study, we have tested whether the supporting material nanohafnia shows any catalytic

activity in hydrogen generation from the hydrolysis of ammonia borane in temperature range used. Control experiments performed starting with 1.0 mmol AB and 20 mg hafnia in 10 mL water at 25.0 or 40.0 ± 0.1 °C show no hydrogen generation in 1 h. This observation clearly indicates that nanohafnia is silent in catalyzing the hydrolysis of ammonia borane in the temperature range used in this study. When ruthenium nanoparticles were supported on hafnia nanopowder, highly active catalysts in hydrogen generation from the hydrolysis of ammonia borane were formed. In fact, Ru^0/HfO_2 catalysts provide high activity in the hydrolysis of ammonia borane generating 3.0 equivalent H_2 gas per mole of AB in the same temperature range.

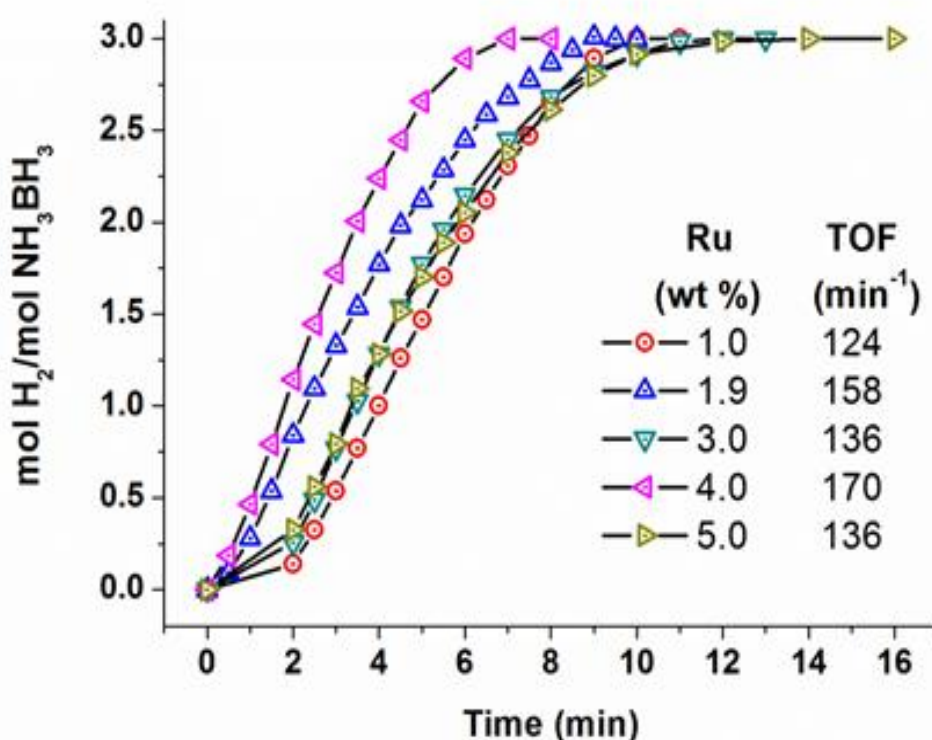


Figure 13. Plot of $\text{mol H}_2/\text{mol H}_3\text{N}\cdot\text{BH}_3$ versus time for the hydrolysis of AB (100 mM) starting with Ru^0/HfO_2 (0.4 mM Ru) with different ruthenium loading at 25.0 ± 0.1 °C.

The catalytic activity of Ru^0/HfO_2 in hydrogen generation from the hydrolysis of ammonia borane at 25.0 ± 0.1 °C was investigated depending on the ruthenium loading of catalyst. Fig. 13 shows the plots of equivalent H_2 gas generated per mole of H_3NBH_3 versus time during the catalytic hydrolysis of 100 mM AB solution using Ru^0/HfO_2 with different ruthenium loading at 25.0 ± 0.1 °C. The hydrogen generation starts after a short induction period less than 2 minutes and continues almost linearly until the consumption of ammonia borane present in the reaction solution. The turnover frequency (TOF) values were calculated from the hydrogen generation rates measured in the linear portion of each plot given in Fig. 13. Note that TOF values refer to the total amount of ruthenium in the catalyst samples and there is no correction for the TOF values by the fraction of catalytically active surface sites. The Ru^0/HfO_2 sample with 4.0% wt. Ru loading provides the highest catalytic activity with a TOF value of 170 min^{-1} in H_2 generation from the hydrolysis of ammonia borane at 25.0 ± 0.1 °C. Therefore, Ru^0/HfO_2 catalyst with a ruthenium loading of 4.0% wt. Ru was used in all of the further experiments performed in this study.

TOF values of the ruthenium catalysts reported in literature for hydrogen generation from the hydrolytic dehydrogenation of ammonia borane are listed in Table 3 for comparison. As clearly seen from the comparison of the values given in Table 3, Ru^0/HfO_2 provides catalytic activity comparable to that of other Ru catalysts in hydrogen generation from the hydrolysis of ammonia borane.

Table 3. The turnover frequency (TOF; $\text{mol H}_2^*/(\text{mol Ru})^{-1}(\text{min})^{-1}$), total turnover number (TON; $\text{mol H}_2/(\text{mol Ru})^{-1}$) and activation energy (E_a ; kJ/mol) values of reported ruthenium catalysts used in hydrogen generation from the hydrolysis of AB at room temperature.

Catalyst	E_a	TOF	Ru/AB ratio	TON	Ref
Ru/graphene	12.7	600	0.002	-	81
Ru/C	34.8	429.5	0.00425	-	82
Ru⁰/CeO₂	51	361	0.00095	135100	83
Ru(0)@MWCNT	33	329	0.00094	26400	84
Ru@SBA-15 NCs	34.8	316	0.002	-	85
Ru/g-C₃N₄	37.4	313	0.0017	-	86
Ru(0)/TiO₂	70	241	0.0006	71500	87
Ru@MIL-96	48	231	0.0039	-	88
Ru/nanodiamond	50.7	229	0.0033	13474	89
Ru@SiO₂	38	200	0.0025	-	90
Ru(0)@PSSA-co-MA	54	180	0.005	51720	91
Ru@MIL-101	51	178	0.008	-	92
Ru(0)/SiO₂-CoFe₂O₄	45.6	172.5	0.00097	-	93
Ru⁰/HfO₂	65	170	0.00396	175600	This study
Ru(0)@Hap	58	137	0.00392	87000	94
Ru/X-NW	77	135	0.00271	134100	95
Ru/graphene	11.7	100	0.010	-	96
Ru@Al₂O₃	46	83.3	0.00375	-	97
Meta stable Ru NPs	27.5	21.8	0.00250	-	98

3.3. Kinetics of Nanohafnia-stabilized Ruthenium(0) Nanoparticles in Hydrogen Generation from the Hydrolysis of Ammonia Borane

Catalytic hydrolysis of ammonia borane was also performed starting with 100 mM AB in the presence of Ru⁰/HfO₂ (0.4 mM Ru) at various temperatures. Figure 14a shows the evolution of equivalent H₂ per mole of AB versus time plots for the hydrolysis of ammonia borane at various temperatures in the range 25.0-40.0 °C. The rate constant for the hydrogen generation was calculated from the slope of the linear part of each hydrogen evolution versus time plot at various temperatures (Figure 14a). From the slope of Arrhenius plot in Figure 14b, activation energy for the hydrolysis of AB catalyzed by Ru⁰/HfO₂ was calculated to be $E_a = 65 \pm 3$ kJ/mol, which is comparable to the literature values listed in Table 3.

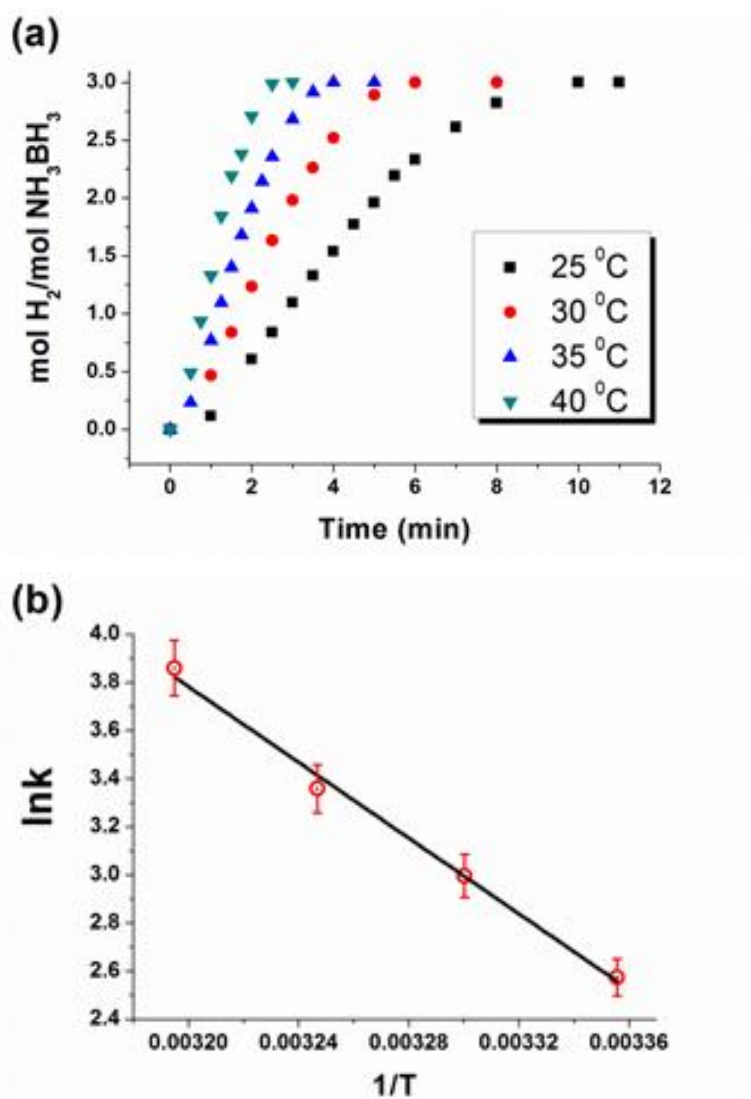


Figure 14. (a) The evolution of equivalent hydrogen per mole of AB versus time plot for the hydrolysis of AB starting with Ru⁰/HfO₂ (0.4 mM Ru) and 100 mM AB at various temperatures. (b) The Arrhenius plot for the Ru⁰/HfO₂ in hydrolysis of AB. $\ln k = -7869(1/T) + 28.96$.

Figure 15a shows the plots of equivalent H_2 gas generated per mole of H_3NBH_3 versus time during the catalytic hydrolysis of 100 mM AB solution using Ru^0/HfO_2 (4.0% wt. Ru) in different catalyst concentration at 25.0 ± 0.1 °C. The hydrogen generation rate was determined from the linear portion of each plot in Figure 15a and plotted versus the initial concentration of ruthenium, both in logarithmic scale, in Figure 15b. The latter logarithmic plot gives straight line with a slope of 0.75 indicating that the catalytic hydrolysis of AB has an order of 0.75 with respect to the ruthenium concentration.

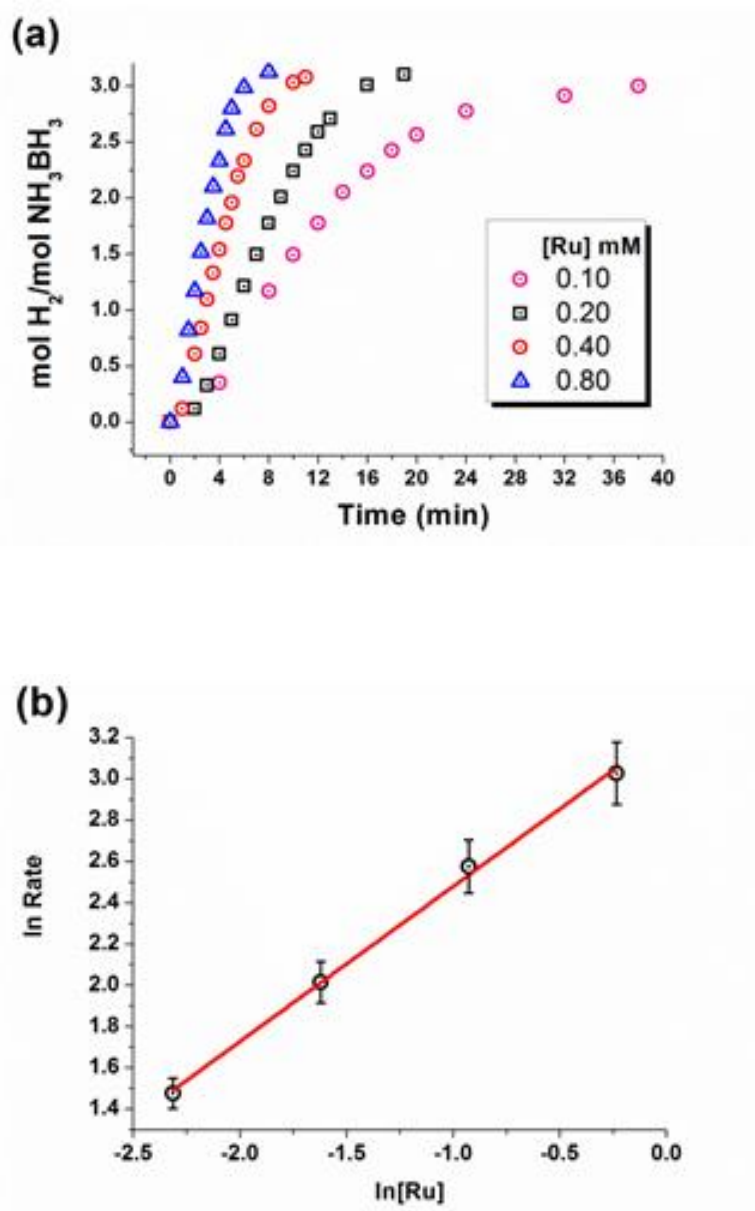


Figure 15. (a) Plots of $\text{mol H}_2/\text{mol H}_3\text{NBH}_3$ versus time depending on the ruthenium concentration in Ru^0/HfO_2 for the hydrolysis of AB (100 mM) at 25.0 ± 0.1 °C. (b) The logarithmic plot of hydrogen generation rate versus the concentration of Ru; $\ln(\text{rate}) = 0.75 \ln[\text{Ru}] + 3.23$.

3.4. Reusability of Ruthenium(0) Nanoparticles Supported on Hafnia in the Hydrolysis of Ammonia Borane

Reusability of Ru^0/HfO_2 catalyst was tested in successive runs of hydrolysis reaction conducted by using the catalyst which have been isolated from the reaction solution following a previous run of hydrolysis of ammonia borane. After H_2 generation from the hydrolysis of ammonia borane was completed, the catalyst was isolated by centrifugation, washed with 50 mL of water and dried under vacuum (10^{-3} torr) at 60°C . The isolated solid sample of Ru^0/HfO_2 was weighed and redispersed in 10 mL solution of 100 mM AB for a subsequent run of hydrolysis which was then started immediately and continued until the completion of H_2 evolution at $25.0 \pm 0.1^\circ\text{C}$. This hydrogen generation process was repeated 5 times in the same way at $25.0 \pm 0.1^\circ\text{C}$. Figure 16a shows the percentage of initial catalytic activity of Ru^0/HfO_2 in the subsequent catalytic hydrolysis of 100 mM AB performed by using catalyst isolated after the previous run of hydrolysis at $25.0 \pm 0.1^\circ\text{C}$. The reusability tests reveal that the Ru^0/HfO_2 catalyst is still active in the subsequent runs of hydrolysis of ammonia borane providing a release of 3.0 equivalent H_2 per mole of AB. After the fifth run of hydrolysis ammonia borane, Ru^0/HfO_2 preserves 75% of their initial catalytic activity. The catalytic activity of the filtrate solution obtained by centrifugation of the solid materials after the fifth run was also tested in the hydrolysis of ammonia borane under the same conditions. The filtrate solution was found to be catalytically silent in hydrogen generation from the hydrolysis of ammonia borane. Therefore, the decrease in catalytic activity in successive runs can be attributed to the agglomeration of nanoparticles on the surface of nanohafnia during the isolation and redispersion processes (Fig. 16b).

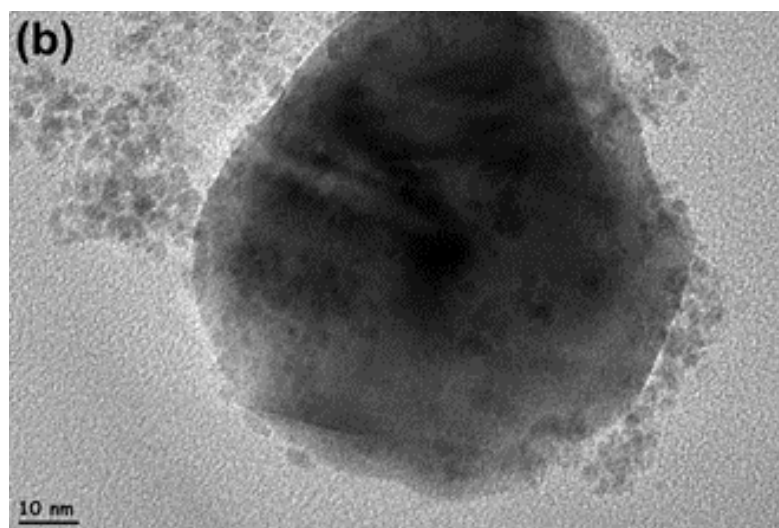
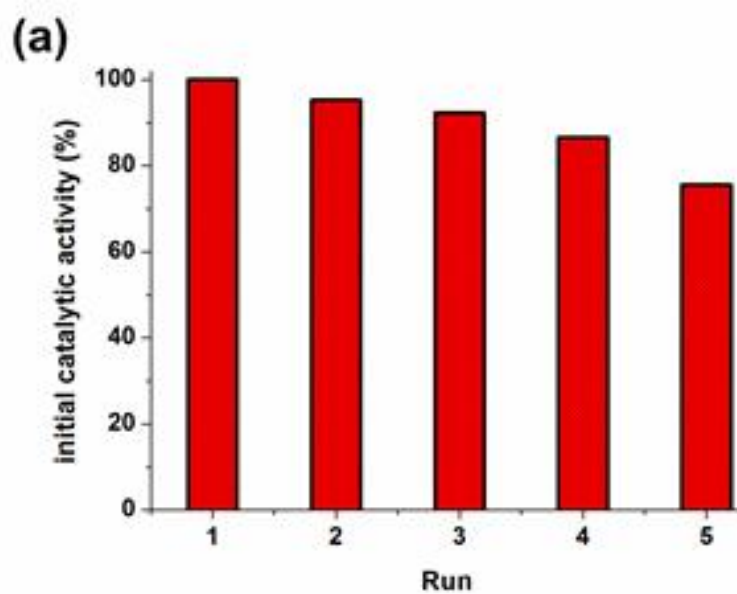


Figure 16. a) Percentage of initial catalytic activity of Ru^0/HfO_2 ($[\text{Ru}] = 158 \text{ mM}$) in successive runs after the reuse for the hydrolysis of AB (100 mM) at $25.0 \pm 0.1 \text{ }^\circ\text{C}$, b) TEM image of Ru^0/HfO_2 sample harvested after fifth run of hydrolysis of AB.

3.5. Catalytic Lifetime of Nanohafnia-stabilized Ruthenium(0) Nanoparticles in Hydrogen Generation from the Hydrolysis of Ammonia Borane

Catalytic lifetime of Ru^0/HfO_2 was determined by measuring the total turnover number (TON) achieved in hydrogen generation from the hydrolysis of ammonia borane. A catalyst lifetime experiment, performed starting with 3.4 mg Ru^0/HfO_2 in 50 mL of solution of AB at 25.0 ± 0.1 °C, reveals a minimum of 175,600 total turnovers over 500 h in hydrogen generation from the hydrolysis of AB before deactivation of the catalyst. Figure 17a shows the variation in turnover number (TON) and turnover frequency (TOF) in the course of reaction. The TOF value decreases expectedly as the ruthenium(0) nanoparticles are deactivated during the lifetime experiment because of the increasing concentration of metaborate ion. As shown in Figure 17b, Ru^0/HfO_2 provides the largest TON value ever reported for hydrogen generation from the hydrolysis of ammonia borane as compared to the other ruthenium catalysts listed in Table 3.

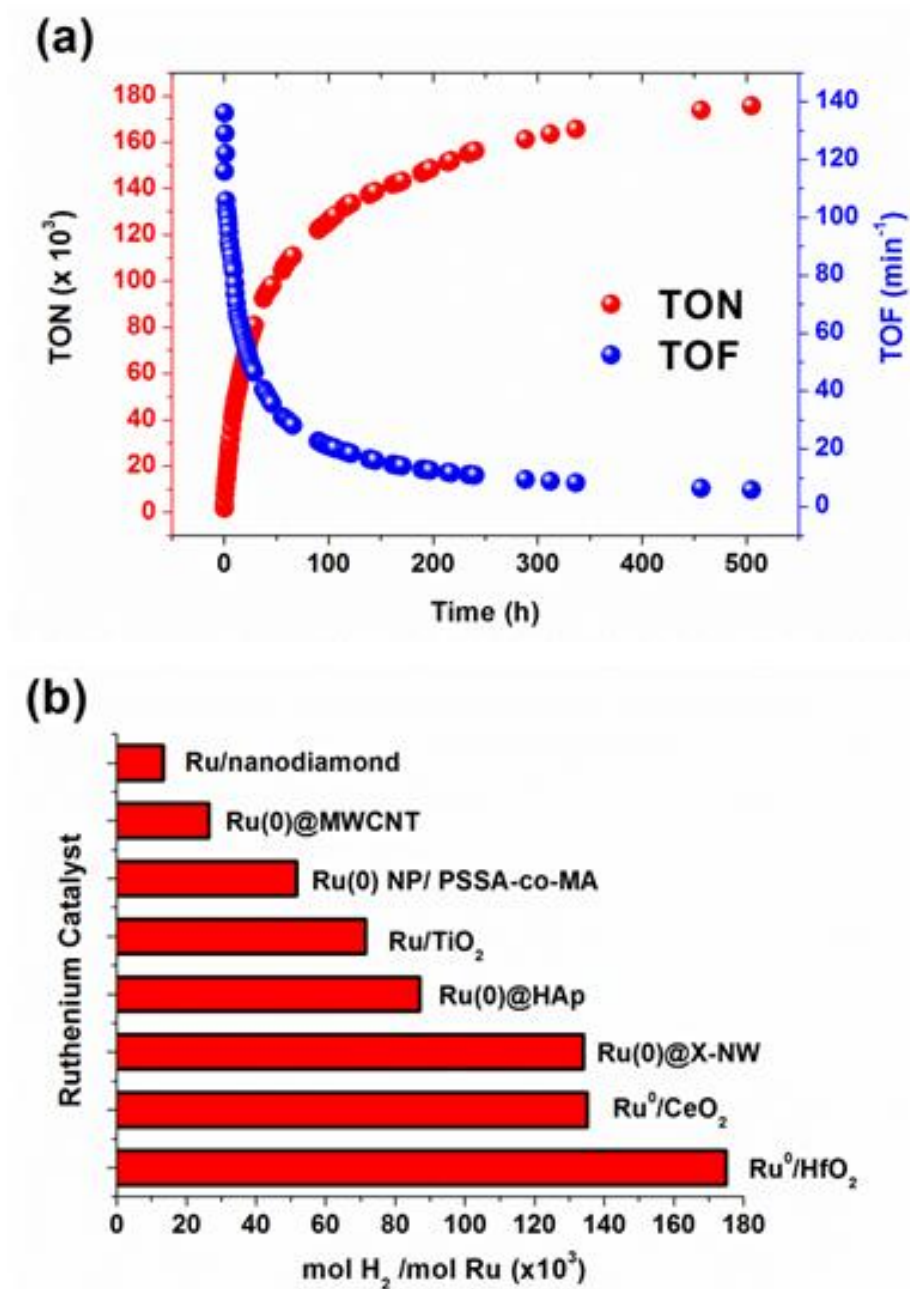


Figure 17. a) The variation in turnover number (TON) and turnover frequency (TOF) during the catalytic lifetime experiment performed starting with 3.4 mg Ru⁰/HfO₂ (4.0% wt Ru, and [Ru] = 0.067 mM) in 50 mL solution of AB at 25.0 ± 0.1 °C, b) Catalytic lifetime of reported ruthenium catalysts (TTO = mol H₂/mol Ru) in the hydrolysis of AB at room temperature.

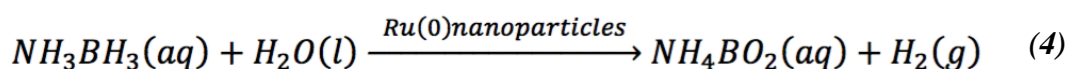
CHAPTER 4

CONCLUSION

This study on the synthesis and characterization of ruthenium(0) nanoparticles supported on nanohafnia as well as on their catalytic use in hydrogen generation from the hydrolysis of ammonia borane reveals the following conclusions and insights.

Highly dispersed ruthenium(0) nanoparticles with particle size in the range 2.4–5.0 nm were reproducibly prepared from the reduction of ruthenium(III) ions impregnated on nanohafnia ($\text{Ru}^{3+}/\text{HfO}_2$) with sodium borohydride in aqueous solution at room temperature and characterized by a combination of advanced analytical techniques.

Ruthenium(0) nanoparticles supported on nanohafnia are highly active catalyst in hydrogen generation from the hydrolysis of ammonia borane at room temperature. The catalytic activity of Ru^0/HfO_2 depends on the ruthenium loading of the Ru^0/HfO_2 sample. The Ru^0/HfO_2 sample with 4.0% wt. Ru loading shows the highest catalytic activity with a TOF value of 170 min^{-1} in hydrogen generation from the hydrolysis of ammonia borane at $25.0 \pm 0.1 \text{ }^\circ\text{C}$ providing a release of 3.0 equivalents of H_2 gas per mole of AB. Ru^0/HfO_2 with 4.0% wt. Ru loading provides unprecedented catalytic lifetime with a total turnover number of $\text{TON} = 175,600$ over 500 h in generation of H_2 from the hydrolysis of ammonia borane at $25.0 \pm 0.1 \text{ }^\circ\text{C}$.



The long lifetime of Ru^0/HfO_2 may be attributed to a favorable metal-support interaction between ruthenium and hafnia nanopowders. It is discernable from the TEM images that ruthenium(0) nanoparticles are well dispersed on the surface of hafnia nanopowders without tightly sticking into the hafnia framework. This makes most of the surface ruthenium sites available for the substrate molecules undergoing the catalytic reaction. This simple facile method developed for the preparation of ruthenium(0) nanoparticles supported on hafnia nanopowders can be extended to other hafnia-based metallic systems in applications in the field of hydrogen generation using ammonia borane.

$\text{Ru}(0)/\text{Hafnia}$ are very attractive catalysts for on-board hydrogen generation from the hydrolysis of ammonia borane in the sense of high catalytic activity, reusability, and simple preparation and isolation procedures.

REFERENCES

- [1] Mazloomi, K.; Gomes, C., Hydrogen as an energy carrier: Prospects and challenges. *Renewable and Sustainable Energy Reviews* **2012**, 16(5), 3024-3033.
- [2] Sources of Greenhouse Gas Emissions, Retrieved March 17, 2016, from Mazloomi, K.; Gomes, C., Hydrogen as an energy carrier: Prospects and challenges. *Renewable and Sustainable Energy Reviews* **2012**, 16(5), 3024-3033.
[1] <https://www3.epa.gov/climatechange/ghgemissions/sources.html>
- [2] Sources of Greenhouse Gas Emissions, Retrieved March 17, 2016, from <https://www3.epa.gov/climatechange/ghgemissions/sources.html>
- [3] United Nations Department of Economic and Social Affairs. World population to 2300, New York: United Nations, Department of Economic and Social Affairs, **2004**.
- [4] Annual Energy Outlook 2015 with Projections to 2040, Retrieved March 3, 2015, from <http://www.eia.gov/forecasts/aeo/>
- [5] Sathre, R., Comparing the heat of combustion of fossil fuels to the heat accumulated by their lifecycle greenhouse gases. *Fuel* **2014**, 115, 674-677.
- [6] U.S. Energy Information Administration - EIA - Independent Statistics and Analysis, Retrieved March 17, 2016, from <http://www.eia.gov/forecasts/aeo/>
- [7] TUSIAD. Evaluation of energy strategy of Turkey towards 21st century [in Turkish]. No. TUSIAD-T/98-12/239, Istanbul, **1998**.
- [8] Armaroli, N.; Blazani, V., The Hydrogen Issue. *ChemSusChem* **2011**, 4 (1), 21-36.
- [9] Olah, G. A.; Goeppert, A.; Prakash, G. K. S., *Beyond Oil and Gas: The Methanol*

Economy, Wiley-VCH, Weinheim, **2006**.

- [10] Ultanir, M. O., Hidrojenin yakit olarak kullanımı ve özellikleri. *Çevre-Enerji Kongresi, TMMOB Makine Mühendisleri Odası* **1997**, 295–315.
- [11] Midilli, A.; Ay, M.; Dincer, I.; Rosen, M. A., On hydrogen and hydrogen energy strategies I: Current status and needs. *Renewable & Sustainable Energy Reviews* **2005**, 9(4), 255-271.
- [12] Olgun, H.; Midilli, A.; Rzaev, P.; Ayhan, T., Pyrolysis studies of nutshells. *Proceedings of 10th International Conference on Thermal Engineering and Thermogrammetry (THERMO), Budapest, Hungary* **1997**, 16–21.
- [13] Midilli, A.; Rzaev, P.; Ayhan, T., Güneş enerjili kapalı çevrimli hidrojen ayrıştırma sistemi. *Güneş Günü Sempozyumu ve Fuarı, İzmir, Türkiye, vol. 1.* **1998**, 34–8.
- [14] Ogden, J., Prospects for building a hydrogen energy infrastructure. *Annu Rev Energy Environ* **1999**, 24, 227–79.
- [15] Verhelst, S.; Wallner, T., Hydrogen-fueled internal combustion engines. *Prog Energy Combust Sci* **2009**, 35, 490–527.
- [16] Jones, M. D., *Towards hydrogen economy. Presented in the IEA Renewable Energy Working Party Seminar*, Paris, March 3. **2003**.
- [17] Rand, D. A. J.; Dell, R. M., *Hydrogen Energy: Challenges and Prospects*, RSC, Cambridge, **2008**.
- [18] Züttel, A.; Borgschulte, A.; Schlapbach, L., *Hydrogen as a Future Energy Carrier*, Wiley-VCH, Weinheim, **2008**.
- [19] Chen, P.; Xiong, Z. T.; Luo, J. Z.; Lin, J. Y.; Tan, K. L., Interaction of hydrogen with metal nitrides and imides. *Nature* **2002**, 420, 302–304.

- [20] Kojima, Y.; Kawai, Y.; Kimbara, M.; Nakanishi, H.; Matsumoto, S., Hydrogen generation by hydrolysis reaction of lithium borohydride. *Int. J. Hydrogen Energy* **2004**, 29, 1213–1217.
- [21] Hamilton, C. W.; Baker, R. T.; Staubitz, A.; Manners, I., B–N compounds for chemical hydrogen storage. *Chem. Soc. Rev.* **2009**, 38, 279–293.
- [22] Singh, S. K.; Zhang, X. B.; Xu, Q., Room-temperature hydrogen generation from hydrous hydrazine for chemical hydrogen storage. *J. Am. Chem. Soc.* **2009**, 131, 9894–9895.
- [23] Demirci, U. B.; Garina, F., Kinetics of Ru-promoted sulphated zirconia catalysed hydrogen generation by hydrolysis of sodium tetrahydroborate. *J. Mol. Catal. A: Chem.* **2008**, 279, 57–62.
- [24] Züttel, A., Hydrogen storage methods. *Naturwissenschaften* **2004**, 91 (4), 157–172.
- [25] Züttel, A., Materials for hydrogen storage. *Materials Today* **2003**, 6 (9), 24–33.
- [26] Langmi, H. W.; McGrady, G. S., Non-hydride systems of the main group elements as hydrogen storage materials. *Coord. Chem. Rev.* **2007**, 251, 925–935; (b) Gutowska, A.; Li, L.; Shin, Y.; Wang, C. M.; Li, X. S.; Linehan, J. C.; Smith, R. S.; Kay, B. D.; Schmid, B.; Shaw, W.; Gutowski, M.; Autrey, T., Nanoscaffold Mediates Hydrogen Release and the Reactivity of Ammonia Borane. *Angew. Chem. Int. Ed.* **2005**, 44, 3578–3582; (d) Demirci, U. B.; Miele, P., Sodium borohydride versus ammonia borane, in hydrogen storage and direct fuel cell applications. *Energy Environ. Sci.* **2009**, 2, 627–637.
- [27] Ramzan, M.; Silvearv, F.; Blomqvist, A.; Scheicher, R. H.; Lebeque, S.; Ahuja, R., Structural and energetic analysis of the hydrogen storage materials LiNH_2BH_3 and NaNH_2BH_3 from ab initio calculations. *Phys. Rev. B* **2009**, 79, 132102–132104.

- [28] Jiang, H. L.; Xu, Q., Catalytic hydrolysis of ammonia borane for chemical hydrogen storage. *Catal Today* **2011**, 170, 56-63.
- [29] Wolf, G.; Baumann, J.; Baitalow, F.; Hoffman, F. P., Calorimetric process monitoring of thermal decomposition of B–N–H compounds. *Thermochim Acta* **2000**, 343, 19-25.
- [30] Zahmakiran, M.; Özkar, S., Metal nanoparticles in liquid phase catalysis; from recent advances to future goals. *Nanoscale* **2011**, 3, 3462- 3481.
- [31] Chandra, M.; Xu, Q., A high-performance hydrogen generation system: Transition metal-catalyzed dissociation and hydrolysis of ammonia–borane. *Journal of Power Sources* 2006, 156 (2), 190-194.
- [32] Xu, Q.; Chandra, M., Catalytic activities of non-noble metals for hydrogen generation from aqueous ammonia–borane at room temperature. *Journal of Power Sources* 2006, 163 (1), 364-370.
- [33] Chandra, M.; Xu, Q., Room temperature hydrogen generation from aqueous ammonia-borane using noble metal nano-clusters as highly active catalysts. *Journal of Power Sources* 2007, 168 (1), 135-142.
- [34] Aiken Iii, J. D.; Finke, R. G., A review of modern transition-metal nanoclusters: their synthesis, characterization, and applications in catalysis. *Journal of Molecular Catalysis A: Chemical* 1999, 145 (1–2), 1-44.
- [35] Çiftçi, N. B.; Metin, Ö., Monodisperse nickel-palladium alloy nanoparticles supported on reduced graphene oxide as highly efficient catalysts for the hydrolytic dehydrogenation of ammonia borane. *Int J Hydrogen Energy* **2014**, 39, 18863-70.
- [36] Chen, W.; Ji, J.; Duan, X.; Qian, G.; Li, P.; Zhou, X.; et al., Unique reactivity in Pt/CNT catalyzed hydrolytic dehydrogenation of ammonia borane. *Chem Commun* **2014**, 50, 2142-4.

- [37] Liang, H. Y.; Chen, G. Z.; Desinan, S.; Rosei, R.; Rosei, F.; Ma, D. L., In situ facile synthesis of ruthenium nanocluster catalyst supported on carbon black for hydrogen generation from the hydrolysis of ammonia-borane. *Int. J. Hydrogen Energy* 2012, 37, 17921–17927.
- [38] Metin, Ö.; Alp, N. A.; Akbayrak, S.; Biçer, A.; Gultekin, M. S.; Özkar, S.; Bozkaya, U., Dihydroxylation of olefins catalyzed by zeolite-confined osmium(0) nanoclusters: an efficient and reusable method for the preparation of 1,2-cis-diols. *Green Chem.* **2012**, 14, 1488-92.
- [39] Rachiero, G. P.; Demirci, U. B.; Miele, P., Bimetallic RuCo and RuCu catalysts supported on γ -Al₂O₃. A comparative study of their activity in hydrolysis of ammonia-borane. *Int J Hydrogen Energy* **2011**, 36, 7051-65.
- [40] Akbayrak, S.; Tonbul, Y.; Özkar, S., Ceria supported rhodium nanoparticles: Superb catalytic activity in hydrogen generation from the hydrolysis of ammonia borane. *Applied Catalysis B: Environmental* **2016**, 198, 162–170.
- [41] Wang, X.; Liu, D.; Song, S.; Zhang, H., Synthesis of highly active Pt–CeO₂ hybrids with tunable secondary nanostructures for the catalytic hydrolysis of ammonia borane. *Chem. Commun.* **2012**, 48, 10207–9.
- [42] Akbayrak, S.; Gençtürk, S.; Morkan, İ.; Özkar, S., Rhodium(0) nanoparticles supported on nanotitania as highly active catalyst in hydrogen generation from the hydrolysis of ammonia borane. *RSC Adv* **2014**, 4, 13742-8.
- [43] Ligthart, D. A. J. M.; Filot, I. A. W.; Almutairi, A. A. H.; Hensen, E. M. J., Identification of step-edge sites on Rh nanoparticles for facile CO dissociation. *Catalysis Communications* **2016**, 77, 5–8.
- [44] Wilk, G. D.; Wallace, R. M.; Anthony, J. M., High-kappa gate dielectrics: Current status and materials properties considerations. *J. Appl. Phys.* **2001**, 89, 5243–5275.

- [45] Villa, I.; Vedda, A.; Fasoli, M.; Lorenzi, R.; Kränzlin, N.; Rechberger, F.; Ilari, G.; Primc, D.; Hattendorf, B.; Heiligt, F. J.; Niederberger, M.; Lauria, A., Size-Dependent Luminescence in HfO₂ Nanocrystals: Toward White Emission from Intrinsic Surface Defects. *Chem. Mater.* **2016**, 28, 3245–3253.
- [46] Wang, J.; Li, H. P.; Stevens, R., Hafnia and hafnia-toughened ceramics. *J. Mater. Sci.* **1992**, 27, 5397-5430.
- [47] Sundqvist, J.; Härsta, A.; Aarik, J.; Kukli, K.; Aidla, A., Atomic layer deposition of polycrystalline HfO₂ films by the HfI₄-O₂ precursor combination. *Thin Solid Films* **2003**, 427, 147-151.
- [48] Aiken III, J. D.; Lin, Y.; Finke, R. G., A Perspective on Nanocluster Catalysis: Polyoxoanion and (n-C₄H₉)₄N⁺ Stabilized Ir(0)~300 Nanocluster "Soluble Heterogeneous Catalysts". *J. Mol. Catal. A: Chem.* **1996**, 114, 29-51.
- [49] Schmid, G. (Ed.), *Clusters and Colloids: From Theory to Applications*, VCH Publishers, New York, **1994**.
- [50] de Jongh, L. J. (Ed.), *Physics and Chemistry of Metal Cluster Compounds*, Kluwer Publishers, Dordrecht, **1994**.
- [51] Vossmeier, T.; DeIonno, E.; Heath, J. R., Light-directed assembly of nanoparticles, *Angew. Chem. Int. Ed Engl.* 36, 1080-1083 (1997).
- [52] Simon, U.; Schön, G.; Schmid, G., The application of Au₅₅ clusters as quantum dots. *Angewandte Chemie International Edition in English* **1993**, 32 (2), 250-254.
- [53] Watzky, M. A.; Finke, R. G., Transition Metal Nanocluster Formation Kinetic and Mechanistic Studies. A New Mechanism When Hydrogen is the Reductant: Slow, Continuous Nucleation and Fast Autocatalytic Surface Growth. *J. Am. Chem. Soc.* **1997**, 119, 10382-10400.
- [54] Schön, G.; Simon, U., A fascinating new field in colloid science: small ligand-

stabilized metal clusters and their possible application in microelectronics. *Colloid and Polymer Science* **1995**, 273 (3), 202-218.

- [55] Antonietti, M.; Göltner, C. G., Superstructures of Functional Colloids: Chemistry on the Nanometer Scale. *Angew. Chem. Int. Ed. Engl.* **1997**, 36, 910–928.
- [56] Reetz, M. T.; Winter, M.; Dumpich, G. ; Lohau, J.; Friedrichowski, S., Fabrication of Metallic and Bimetallic Nanostructures by Electron Beam Induced Metallization of Surfactant Stabilized Pd and Pd/Pt Clusters. *J. Am. Chem. Soc.* **1997**, 119, 4539-4540.
- [57] Elghanian, R.; Storhoff, J. J.; Mucic, R. C. ; Letsinger, R. L.; Mirkin, C. A., Selective Colorimetric Detection of Polynucleotides Based on the Distance-Dependent Optical Properties of Gold Nanoparticles. *Science* **1997**, 277, 1078-1081.
- [58] Sonti, S. V.; Bose, A., Cell separation using protein-A-coated magnetic nanoclusters. *Journal of colloid and interface science* **1995**, 170 (2), 575-585.
- [59] Colvin, V. L.; Schlamp, M. C.; Alivisatos, A. P., Light-emitting diodes made from cadmium selenide nanocrystals and a semiconducting polymer. *Nature* **1994**, 370, 354–357.
- [60] Pool, R., Clusters: strange morsels of matter. *Science* **1990**, 248, 1186–1188.
- [61] Schmid, G.; Maihack, V.; Lantermann, F.; Peschel, S., Ligand-stabilized metal clusters and colloids: properties and applications. *J. Chem. Soc. Dalton Trans.* **1996**, 5, 589-595.

- [62] Aiken III, J. D.; Finker, R. G., A review of modern transition-metal nanoclusters: their synthesis, characterization, and applications in catalysis. *Journal of Molecular Catalysis A: Chemical* **1999**, 145, 1–44.
- [63] Hunter, R. J., *Foundations of Colloid Science*, Vol. 1, Oxford Univ. Press, New York, **1987**.
- [64] Bard, A. J.; Faulkner, L. R., *Electrochemical Methods: Fundamentals and Applications*, 2nd Edition, Wiley, New York, **2001**.
- [65] Napper, D. H., *Polymeric Stabilization of Colloidal Dispersions*, Academic Press, London, **1983**.
- [66] Schmid, G., *General Introduction. In Clusters and Colloids*, Wiley-VCH Verlag GmbH, **2007**, 1-4.
- [67] Bonnemann, H.; Braun, G.; Brijoux, W.; Brinkmann, R.; Schulze Tilling, A.; Seevogel, K.; Siepen, K., *J. Organomet. Chem.* 520 **1996**, 143 – 162.
- [68] Hirtzel, C. S.; Rajagopalan, R., *Colloidal Phenomena: Advanced Topics*, **1985**, pp. 27–39, pp. 73–87.
- [69] Schmid, G. (Ed.), *Clusters and Colloids: From Theory to Applications*, VCH Publishers, New York, **1994**.
- [70] Lin, Y.; Finke, R. G., Novel Polyoxoanion- and BudN⁺-Stabilized, Isolable, and Redissolvable, 20-30-AIr-300-goo Nanoclusters: The Kinetically Controlled Synthesis, Characterization, and Mechanism of Formation of Organic Solvent-Soluble, Reproducible Size, and Reproducible Catalytic Activity Metal Nanoclusters. *J. Am. Chem. Soc.* **1994**, 116, 8335-8353.
- [71] Schmid, G., Clusters and colloids: bridges between molecular and condensed material. *Endeavour, New Series* **1990**, 14, 172–178.

- [72] Watzky, M. A.; Finke, R. G., Transition Metal Nanocluster Formation Kinetic and Mechanistic Studies. A New Mechanism When Hydrogen Is the Reductant: Slow, Continuous Nucleation and Fast Autocatalytic Surface Growth. *J. Am. Chem. Soc.* **1997**, 119, 10382-10400.
- [73] Iwasawa, Y. (Ed.), *Tailored Metal Catalysts*, Kluwer, Dordrecht, **1986**.
- [74] Smith, G. V.; Notheisz, F., *Heterogeneous Catalysis in Organic Chemistry*. Academic Press, San Diego, **1999**.
- [75] Özkar S., Enhancement of catalytic activity by increasing surface area in heterogeneous catalysis. *Appl. Surf. Sci.* **2009**, 256, 1272-1277.
- [76] Richards, R. M., *Surface and Nanomolecular Catalysis*, Taylor & Francis, Boca Raton, **2006**.
- [77] Acar, F. A., *Ruthenium(0) Nanoparticles Supported on Graphene: Preparation, Characterization and Catalytic Use in Hydrogen Generation from Hydrolysis of Ammonia Borane*, **2015**.
- [78] Shen, J. Y.; Adnot, A.; Kaliaguine, S., An ESCA study of the interaction of oxygen with the surface of ruthenium. *Appl. Surf. Sci.* **1991**, 51, 47- 60.
- [79] Suñol, J. J.; Bonneau, M. E.; Roué, L.; Guay, D.; Schulz, R., XPS surface study of nanocrystalline Ti–Ru–Fe materials. *Appl. Surf. Sci.* **2000**, 158, 252-262.
- [80] Wagner, C. D.; Muilenberg, G. E.; Riggs, W. M.; Davis, L. E.; Moulder, F. J., *Handbook of X-ray photoelectron spectroscopy; physical electronic division*. Perkin-Elmer, 55, **1979**.
- [81] Du, C.; Ao, Q.; Cao, N.; Yang, L.; Luo, W.; Cheng, G., Facile synthesis of monodisperse ruthenium nanoparticles supported on graphene for hydrogen generation from hydrolysis of ammonia borane. *International Journal of Hydrogen Energy* **2015**, 40, 6180-7.

- [82] Liang, H. Y.; Chen, G. Z.; Desinan, S.; Rosei, R.; Rosei, F.; Ma, D. L., In situ facile synthesis of ruthenium nanocluster catalyst supported on carbon black for hydrogen generation from the hydrolysis of ammonia-borane. *Int. J. Hydrogen Energy* **2012**, 37, 17921–17927.
- [83] Akbayrak, S.; Tonbul, Y.; Özkar, S., Ceria-Supported Ruthenium Nanoparticles as Highly Active and Long-Lived Catalyst in Hydrogen Generation from the Hydrolysis of Ammonia Borane. *Dalton Trans.* **2016**, DOI: 10.1039/C6DT01117A.
- [84] Akbayrak, S.; Özkar, S., Ruthenium(0) nanoparticles supported on multiwalled carbon nanotube as highly active catalyst for hydrogen generation from ammonia-borane. *ACS Appl Mater Interfaces* **2012**, 4, 6302-10.
- [85] Yao, Q.; Lu, Z. H.; Yang, K.; Chen, X.; Zhu, M., Ruthenium nanoparticles confined in SBA-15 as highly efficient catalyst for hydrolytic dehydrogenation of ammonia borane and hydrazine borane. *Sci. Rep.* **2015**, 5, 15186-96.
- [86] Fan, Y.; Li, X.; He, X.; Zeng, C.; Fan, G.; Liu, Q.; Tang, D., Effective hydrolysis of ammonia borane catalyzed by ruthenium nanoparticles immobilized on graphitic carbon nitride. *Int. J. Hydrogen Energy* **2014**, 39, 19982-9.
- [87] Akbayrak, S.; Tanyıldızı, S.; Morkan, İ.; Özkar, S., Ruthenium(0) nanoparticles supported on nanotitania as highly active and reusable catalyst in hydrogen generation from the hydrolysis of ammonia borane. *International Journal of Hydrogen Energy* **2014**, 39, 9628-9637.
- [88] Wen, L.; Su, J.; Wu, X.; Cai, P.; Luo, W.; Cheng, G., Ruthenium supported on MIL-96 An efficient catalyst for hydrolytic dehydrogenation of ammonia borane for chemical hydrogen storage. *Int. J. Hydrogen Energy* **2014**, 39, 17129-17135.

- [89] Fan, G.; Liu, Q.; Tang, D.; Li, X.; Bi, J.; Gao, D., Nanodiamond supported Ru nanoparticles as an effective catalyst for hydrogen evolution from hydrolysis of ammonia borane. *Int. J. Hydrogen Energy* **2016**, 41, 1542-49.
- [90] Yao, Q. L.; Shi, W. M.; Feng, G.; Lu, Z. H.; Zhang, X. L.; Tao, D. J., Ultrafine Ru nanoparticles embedded in SiO₂ nanospheres: highly efficient catalysts for hydrolytic dehydrogenation of ammonia borane. *J. Power Sources* **2014**, 257, 293-299.
- [91] Metin, Ö.; Sahin, S.; Özkar, S., Water-soluble poly(4-styrenesulfonic acid-co-maleic acid) stabilized ruthenium(0) and palladium(0) nanoclusters as highly active catalysts in hydrogen generation from the hydrolysis of ammoniaborane. *Int J Hydrogen Energy* **2009**, 34, 6304-13.
- [92] Cao, N.; Liu, T.; Su, J.; Wu, X.; Luo, W.; Cheng, G., Ruthenium supported on MIL-101 as an efficient catalyst for hydrogen generation from hydrolysis of amine boranes. *New J. Chem.* **2014**, 38, 4032-4035.
- [93] Akbayrak, S.; Kaya, M.; Volkan, M.; Özkar, S., Ruthenium(0) nanoparticles supported on magnetic silica coated cobalt ferrite: Reusable catalyst in hydrogen generation from the hydrolysis of ammonia-borane. *J. Mol. Catal. A Chem.* **2014**, 394, 253-261.
- [94] Akbayrak, S.; Erdek, P.; Özkar, S., Hydroxyapatite supported ruthenium(0) nanoparticles catalyst in hydrolytic dehydrogenation of ammonia borane: insight to the nanoparticles formation and hydrogen evolution kinetics. *Appl Catal B: Environ* **2013**, 142-143, 187-95.
- [95] Akbayrak, S.; Özkar, S., Ruthenium(0) nanoparticles supported on xonotlite nanowire as long-lived catalyst for hydrolytic dehydrogenation of ammonia borane. *Dalton Trans.* **2014**, 43, 1797-805.

- [96] Cao, N.; Luo, W.; Cheng, G., One-step synthesis of graphene supported Ru nanoparticles as efficient catalysts for hydrolytic dehydrogenation of ammonia borane. *Int J Hydrogen Energy* **2013**, 38, 11964-72
- [97] Can, H.; Metin, Ö., A facile synthesis of nearly monodisperse ruthenium nanoparticles and their catalysis in the hydrolytic dehydrogenation of ammonia borane for chemical hydrogen storage. *Appl. Catal. B* **2012**, 125, 304-310.
- [98] Abo-Hamed, E. K.; Pennycook, T.; Vaynzof, Y.; Toprakcioglu, C.; Koutsioubas, A.; Scherman, O. A., Highly Active Metastable Ruthenium Nanoparticles for Hydrogen Production through the Catalytic Hydrolysis of Ammonia Borane. *Small* **2014**, 10, 3145–52.